NONHLANHLA
FUNGURA

INTEGRATION OF COMMINUTION AND LEACHING PROCESSES USING THE ATTAINABLE REGIONS ANALYSIS

This dissertation is submitted to the Faculty of Engineering and the Built Environment, University of Witwatersrand, in fulfillment of the requirements of the degree of Master of Science.

Johannesburg, 2010

DECLARATION

I declare that this dissertation is my own work (except for the referenced portions). It is being submitted for the degree of Master of Science in the University of Witwatersrand, Johannesburg. It has not been submitted before for any degree or examination in any other university.

.....

Nonhlanhla Fungura

10 June 2011

ABSTRACT

In this study, the researcher considers leaching and comminution units as one processing system, using the population balance model of comminution and the shrinking core model of leaching to develop a model for a combined system. Comminution is often operated with a target size derived independently of considerations of the optimal requirements of downstream processing operations. This research, however, proposes an integrated processing model that can be used to predict the particle size distribution required to achieve a targeted output from the comminution and leaching processes.

Process engineers have traditionally modeled and optimized the unit operations of comminution and leaching separately, within an overall flow sheet. The research described in this thesis models the comminution breakage process and the leaching processes to optimize the overall combined system. This framework offers the advantages of improving the operating efficiency of systems; reducing energy consumption, wastes and negative environmental impacts; and maximizing mineral recovery. More efficient processes will also make the industries based on extractive metallurgy more profitable.

To my baby girl Thabisile and all my future offspring.

ACKNOWLEDGEMENTS

I would like to the thank my supervisors Professor Hildebrandt, Dr Ndlovu, Dr Khumalo and Professor Glasser for their invaluable support and all the ideas that contributed to the success of the dissertation.

I would also like to thank my colleagues in the COMPS Comminution Research Group for the academic and social support

I would also like to acknowledge the financial support from COMPS and Postgraduate Merit Award

Special thanks go to my husband for the support every step of the way

Above all, I thank God for without Him nothing would have been possible

Table of Contents

CHAPTER ONE - INTRODUCTION

A wide range of mineral processing operations are employed to liberate and recover minerals from ores. It is generally the goal of these operations to recover the greatest possible amount of minerals at the least possible cost. Typically research has focused on optimizing individual unit operations rather than looking at the overall flow sheet, which shows the interactions between the individual units, and their eventual integration. The development of an integrated approach to mineral processing systems and flow sheets is intended to create a methodology for process synthesis that can be applied throughout the extractive metallurgical industry. The improved efficiency resulting from an approach that integrates the processes will help to bring about optimum mineral recovery, and a reduction in energy consumption, waste products, and harm to the environment. In general, these advantages will contribute to the benefit of society.

1.1 BACKGROUND

Various researchers have developed mathematical models to predict the behavior and the outcomes of mineral processing operations. These are used to design and operate mineral processing circuits efficiently. This study aims to create a new approach to modeling and optimizing comminution and leaching processes, using the population balance and shrinking core models, and applying attainable regions analysis to study process optimization with a view to achieving a higher rate of mineral recovery, a shorter production time and lower energy consumption for the overall system.

Comminution is one of the four main groups of mechanical procedures that are applied in chemical and mineral processing. This term refers to methods of crushing or grinding that reduce

particles of various dimensions into much smaller sizes. (The other three forms of operation are agglomeration, separation and mixing.) Comminution can be found in everyday activities, for example cooking, when a pepper mill or a grater is used in the preparation of different foodstuffs. Other industrial applications are found in biomass processing, the preprocessing of cellulosic material to produce ethanol, mineral processing (the extraction of raw materials), the production of food, cement, ceramic and chemical goods, and the processing of waste. In most of the cases, the word "comminution", is used with reference to solids. The distinction made between crushing and grinding in comminution is dependent on the particle size: crushing applies to coarse feed materials (bigger than 50–100 mm), and grinding to materials finer than 50 mm.

Leaching is the primary extractive operation in hydrometallurgical processing. It can be generally described as a process by which a metal or a specific mineral is transferred from a matrix containing naturally-occurring minerals into an aqueous solution. The most common models of the leaching process are the shrinking core and shrinking particle approaches, which have been used successfully to design and simulate the leaching process in various extractive contexts.

Every year, vast tonnages of metals of immense value are produced in whole or in part through the hydrometallurgical leaching process. For example, increasing amounts of copper and almost all the gold and platinum group metals as well as the base metals zinc, lead and nickel, are treated in this manner. The basic steps that incorporate leaching to extract various metals from ore are dissolution (or leaching); elimination of unwanted material from the pregnant solution by (for example) filtration; concentration of the values; and their removal from the solution by

means such as chemical precipitation or reduction of the metal, whether chemically or electrochemically.

It is obviously of paramount importance that the specific mineral should be made soluble in water or in some other inexpensive lixiviate, such as sulphuric acid. This generally requires that the ore is subjected to pre-treatment to render the mineral accessible to the solvent, and chemically dissoluble. Thus, pre-treatment usually involves the crushing followed by the grinding of the ore to a particle size that renders it capable of being leached within an appropriate period. Leaching is also increasingly used as an intermediate process that is applied to the crushed products of various smelting operations. After the chosen metal has been dissolved, it is subjected to the appropriate extraction processes.

1.2 OBJECTIVES OF THE WORK

1.2.1 Objectives

The following are the objectives of the project:

- to consider comminution and leaching using the population balance and the shrinking core models;
- to optimize an integrated comminution and leaching system with various objective functions, using attainable regions analysis;
- to produce recommendations and conclusions using data obtained from the mathematical process model.

1.2.2 Hypothesis

In order to obtain the greatest advantage from the whole process of extracting metals and minerals, the comminution and leaching processes must be regarded parts of an overall system. By developing an integrated system the researcher aims to make it possible for the metallurgical industry to recover higher volumes of minerals while reducing both production time and energy consumption.

1.3 DISSERTATION OUTLINE

The dissertation is divided into four chapters. The first comprises an introduction to the project, and gives an overview of the whole report.

Chapter 2 covers the fundamentals of comminution, provides a background to the various comminution processes, and deals with both the literature on comminution circuits and various models that have been developed to predict the way such circuits behave. Many models have been postulated to explain how particle size changes as comminution proceeds. These are reviewed in this chapter, but detailed attention is given to the population balance model and the attainable region (AR) analysis of the comminution circuit. In Chapter 2 the writer also discusses leaching models, particularly the shrinking core and shrinking particle models. The former is of particular interest to this study, and is therefore examined in considerable detail. It is generally regarded as the model that most realistically represents the leaching that occurs in most mineral processing operations. The AR approach is also discussed, as a geometric tool that develops a convex candidate attainable region using fundamental processes. The writer presents a simple

system with reaction and mixing, which illustrates the application of this approach to chemical engineering.

The model of a combined integrated comminution and leaching process, based on a typical zinc sulphide leaching system developed by Aydogan et al (2005), is developed and discussed in Chapter 3. The author also demonstrates and explains the sensitivity/responsiveness of the model to changes in the control regime and leaching time. The candidate AR is constructed for the first-order reaction system. Also, because selectivity is an important aspect of leaching, an investigation and analysis of the selectivity of two mineral species in the integrated leach system is provided.

Chapter 4 presents the conclusions the researcher arrived at on the basis of the work done. It also discusses the applicability to mineral processing systems of the type of model developed, and makes recommendations for the line that future research should follow.

CHAPTER TWO – REVIEW OF EARLIER RESEARCH INTO MODELING AND OPTIMISING COMMINUTION AND LEACHING SYSTEMS

2.1 INTRODUCTION

The task of process synthesis is to develop the most efficient way to manufacture a particular product (or set of products) from an available raw material. The optimal process is determined by the outcome that is of specific interest to the process engineer. Criteria such as process yield, energy efficiency, product selectivity and waste minimization are significant to the designing of a particular process, and all contribute to the ultimate objective of reducing the overall cost of producing the mineral concerned.

In this chapter we look at the history of comminution and leaching, which are among the most important procedures in the mineral processing field. Attainable regions analysis, as well as process integration, uses these models in order to optimize the overall comminution- leaching system.

2.2 COMMINUTION

Comminution is a unit operation of primary importance to modern industry. The term is used to describe a collection of physical processes that can be applied to ores to reduce the size of the particles in a stream. Comminution may take many different forms, which include crushing and grinding, and separating particles into streams of different sizes by means of screens and other

classification devices. The major purpose of comminution is to convert certain raw materials into more saleable or useable products, or to prepare them for further processing. Also, there is an aspect of comminution that is common to most industrial processes, particularly those associated with the extraction of metals from minerals: it is energy-intensive. Therefore any improvement in the energy efficiency of communition processes, for example in milling, offers an opportunity to increase overall profitability.

2.2.1 Grinding Theory

Particles are broken up through the appropriate application of energy, whether kinetic, compression, microwave and/or chemical. One of the earliest theories of comminution, developed in 1867 by Peter Ritter Von Rittinger, dealt with the relationship between energy input and the breakage of particles. He postulated that the energy input to a particle is proportional to the new surface area produced. (Equation 2.1 below is the mathematical representation of this theory.) His formulation proposes that a certain amount of energy is required to break the bonds between two particles.

$$E_r = K_r[\text{new surface area} - \text{old surface area}] \qquad (2.1),$$

where K_r is the grinding rate and E_r is the specific energy input.

A shortcoming in Rittinger's hypothesis is that it does not account for the fact that particles absorb energy elastically before they reach their yield point: thus, during grinding, the energy supplied goes not only into new surface generation, but also into elastic energy, heat and noise.

Experimental work done by Rose in 1967 [1] showed that the energy required for new surface generation is less than 1% of the power supplied to the mill.

In 1885 Fredrich Kick developed the second theory of comminution, which states that the amount of deformation of the particles is proportional to the amount of energy applied. This resulted in the energy/size reduction hypothesis attributed to Kick: "For any unit weight of ore particles, the energy required to produce any given reduction ratio in the volume is constant no matter what may be the original size of the particles" [1]. This can be represented mathematically by equation 2.2:

$$E_k = K_k [x_f/x_p] \qquad (2.2),$$

where E_k is the specific energy required to reduce feed particles of size x_f to product particles of size x_p, and K_k is the rate constant.

A third explanation of comminution was published by Fred Bond in 1952[1]. He postulated that the energy used in breaking a stated weight of homogeneous material is inversely proportional to the square root of the diameter of the product particles. The mathematical representation of the theory is given as follows (equation 2.3):

$$E_b = K_b \left[\frac{10}{x_p^{0.5}} - \frac{10}{x_f^{0.5}} \right] \qquad (2.3),$$

where K_b is the bond proportionality constant.

The Bond hypothesis suggests that work input is used in the deformation of the particles and that this is released as heat. Local deformations beyond the critical strain result in the formation of a crack, which propagates and results in breakage. The strain energy levels depend on the volume of the particle, while the expansion of the crack results in the creation of new surface area. As should be apparent, Bond's postulation combines those of Rittinger and Kick. The Bond theory has found extensive application in comminution systems for the quantitative definition of the resistance of solid particles to breakage. Its major shortcoming is, however, that it groups all the grinding sub-processes into a single work index term, which limits its validity and application [1].

These theories of comminution are empirically based, which imposes constraints on their usefulness to the engineer designing comminution systems. For example, they cannot be applied to wide size distribution, the sub-processes of transportation, normalization of the distribution of breakage products, and selectivity. The population balance model was developed to address these limitations, and to provide a matrix that could be applied to the many different aspects of comminution, and could also be used for quantitative modeling.

2.2.2 The Population Balance Model

The characterization of a particle population through the distribution of particles in the external and internal variable space provides a powerful formalized modeling procedure. When the particles move in the phase space they are altered in terms of their size. It is essential that the particles are classified according to their characteristics and their interaction with one another. The particle size mainly influences the classification of particles, in addition mineralogical

composition, chemical composition, particle shape and surface specific energy can also be of influence. There are some influencing characteristics such as mineralogical composition that can be multidimensional. If there are more than two minerals in the particles the mineralogical vector must include one coordinate for each distinct mineral.

The population balance model developed by Reid in 1965 can be used effectively to predict comminution behavior, because it takes into account all the sub-processes of breakage kinetics, material transport and size classification. According to this formula, the feed material is ground for a set time (t), a known sample is removed, and the fraction within the original size interval is determined by sieving and weighing. The sample is returned to the mill, which is run for an additional time (t_2) and reanalyzed. The rate of disappearance of the mass is in a certain size class is proportional to the amount of mass in that size class, as represented in equation 2.4 below:

$$-\frac{dm_i(t)}{dt} \alpha \quad m_i(t)M \qquad (2.4),$$

where M is the total mass and is constant, and m_i is the mass fraction of material in size class i.

Introducing a proportionality constant (S_i) yields equation 2.5, where S_i represents the specific rate of breakage:

$$m_i(t) = m_i(0)\exp(-S_i t) \qquad (2.5),$$

When a sample is ground; the process results in a wide range of product sizes and the distribution of material in the various size classes changes as the milling progresses. Primary breakage occurs when the material is ground up, and the fragments produced are mixed back into the general mass of the material in the mill. If the material of size class 1 (the largest in size) is broken up, the weight fraction of the products that occurs in the size interval *i* is called b_{i1}. The set of numbers b_{i1}, that is, those referring to a descending order of sizes from class 1 from class size 2 onward to n, then describes the distribution of fragments. Normally the matrix of numbers b_{ij} is needed to describe the general fragmentation into all sizes of interest. The rate of production of size class i material is equal to both the product of the fraction of *i* from *j*, and the rate of breakage of size *j*. This concept is used in the formulation of the equations relating to grinding. Particles in size class *j* are broken into smaller sizes, with every fragment of whatever size contributing to the diminishing scale of the particles as comminution proceeds. The net rate of production of size *i* material equals the sum of the rate of appearance from breakage of all larger sizes minus the rate of disappearance by breakage. This concept is represented by equation 2.6:

$$\frac{dm_i(t)}{dt} = -S_i m_i(t) + \sum_{j=i}^{i-1} S_j b_{ij} m_j \qquad (2.6),$$

where $m_i(t)$ is the mass fraction of the particles in the *i*th size class interval at time *t*, S_i the breakage rate function of size class *i*, b_{ij} is the breakage distribution function, and *t* is the time.

Therefore in order to model the comminution process, two sets of coefficients are introduced, the rate of breakage and the distribution.

a) The rate of breakage (S_i) describes the proportion of particles leaving the class *i* by comminution per unit time.

b) Distribution (b_{ij}) describes the amounts of each size of fragments, with b_{ij} corresponding to the proportion that reaches size class *i* when particles of size *j* are ground.

The population balance model postulates that the particle size interval is divided into as many narrow particle size fractions, n, as possible, with the first fraction (i=1) containing the coarsest whilst the last fraction (i=n) contains the finest particles. The mass fraction of the class *i* is called m_i; thus $\Sigma m_i = 1$.

The conditions for classifying particles as belonging to a size class *i* are:

$$m_{i+1} < m \leq m_i$$

and always

$$m_i < m_j \quad \text{for } i > j.$$

For the purposes of this investigation, we consider three size classes: the feed class (size 1), the median (size 2), and the fine (size 3). Equations 2.7 and 2.8 describe the change in mass of size classes 1 and 2 over time. The alteration in mass fraction of size class 3 is found by using the mass balance of the system, on the assumption that mass is conserved. (See equation 2.9.)

$$\frac{dm_1(t)}{dt} = -S_1 m_1(t) \qquad (2.7),$$

$$\frac{dm_2(t)}{dt} = -S_2 m_2(t) + S_1 b_{21} m_1(t) \qquad (2.8),$$

Based on the conservation of mass therefore:

$$m_3 = 1 - (m_2 + m_3) \qquad (2.9),$$

For simulation of the population balance model comminution in grinding mill, the selection and the breakage functions are created and combined in a mill matrix. This mill matrix is multiplied by the feed matrix which describes the particle size distribution entering the mill. The multiplication yields the mill product matrix which describes the size distribution of the feed and product.

The population balance equation provides a powerful model for the description of industrial comminution machines. It allows the development of a uniform model that describes the operating behavior of rod, ball, semi autogenous and autogenous mills. The popular form of the population model that is usually used as the restricted form 2.6. This form has its drawbacks in that it can only be used for one internal coordinate; the particle size and it is assumed that the breakage and wear processes are not dependent on the position of the particle in the mill so external factors that affect breakage are not considered.

2.3 LEACHING

Crundwell [7] describes leaching as a unit operation that is central to the hydrometallurgical treatment of ores. It is one of the downstream processes that occur in mineral processing, and is commonly used in the recovery of; *inter alia*, copper, nickel, cobalt, zinc and uranium from the ores that contain them. Efficient leaching results in the maximum recovery of a metal of interest.

Leaching is the operation that follows comminution, which ensures that the ore is finely ground to liberate the leachable material. During leaching, which can be defined as the process of extracting a soluble constituent from a solid by means of a solvent, the main purpose is to dissolve as much of the soluble material as possible.

A number of formulae have been used to predict the behavior of fluid–solid systems. The shrinking core, shrinking particle, homogeneous and grain models are the most commonly-used descriptions for non-catalytic fluid–solid reactions. Modeling a leaching system requires several assumptions to make the system "ideal". The solubility of solute may have an upper bound, limiting how much solute the solvent may hold. Ideally, the carrier will not dissolve, and so will not be present in the overflow. This is a generally safe assumption, although allowance should be made for entrainment of solid flakes, etc., in the overflow from the first stage.

Mixing of the solid and the solvent is critical. Typically, "perfect mixing" is assumed, as the idea of an equilibrium stage (the solid and liquid phases on each stage are in equilibrium). These assumptions imply that all the liquid within the stage has the same composition and so the

overflow and the liquid carried in the underflow are identical. This is known as the uniform solution assumption and will result in a linear equilibrium curve.

One also needs to determine how much liquid leaves entrained with the solids in the underflow. The simplest option is the assumption of constant solution underflow which means that every stage has the same, fixed ratio of solution to solid in the underflow stream. Like the equimolar overflow assumption in distillation, this will produce a linear operating curve. The first stage is again problematic, since it must "wet" the solid (fill pores, etc.) and so will typically pick up more liquid than subsequent stages.

More generally, the amount of solution in the underflow depends on the properties of the solution, which are dependent on its composition. The amount of solute present seems to effect the "stickiness" of the solution. As a result, "draining data" is typically collected. This relates the solution/solid ratio to the composition of the solution and is used to determine the nature of the operating curve.

The shrinking core model is applied in cases where the particles are initially non-porous, on the assumption that one party to the reaction in the solid particle reacts with the solvent (the other party), creating a layer surrounding the core of the particle, which has not reacted. The shrinking particle model is similar, but it postulates that no product layer is formed around the un-reacted core. The grain models are used for solids that have individual grains densely compacted together, while the homogeneous model is applicable to particles in which the distribution of pores is consistent throughout (homogeneous).

2.3.1 The Shrinking Core Model

The shrinking core model, which was first postulated by Yagi and Kunni in 1955, [20] is widely used for predicting the kinetics of mineral dissolution in hydrometallurgy in general and leaching systems in particular. The leaching of mineral particles by means of a reagent in solution can be represented by the following equation:

$$A(g) + bB(solid) \longrightarrow \text{aqueous and solid products} \qquad (2.10),$$

where A represents the soluble component undergoing leaching, B represents the solvent, and b is the stoichiometric coefficients of B.

This formulation, which represents a reaction, is the basis of the shrinking core model, which postulates that as the reaction proceeds, the solid component is converted into a soluble product and some other solid waste material, which is left behind as an un-reacted solid, an 'ash' that is porous and inert. The un-reacted core shrinks as the reaction progresses, whilst the overall size of the particles remains constant.

The model is constructed on the following assumptions:

- the solid particles undergoing leaching have a spherical geometry and are non-porous at the start of, and during, the reaction;
- the chemical reaction is irreversible and first-order with respect to the liquid reactant;

- the chemical reaction determines the kinetics of the whole process;
- the concentration of the lixiviate is constant throughout the whole process.

The leaching process is illustrated in Figure 2.1 below

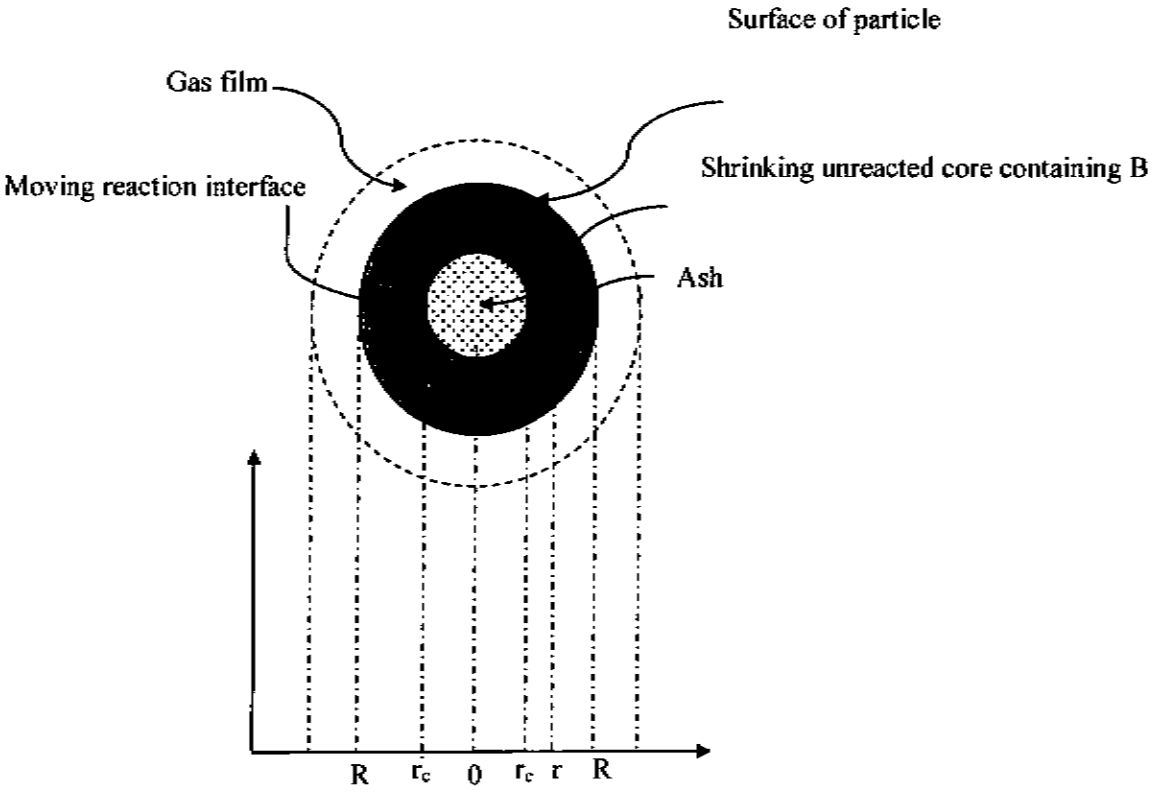

Figure 2.1. Representation of concentrations of reactants and products for the reaction A(g)+bB(s)↔aqueous and solid products for a particle of unchanging size (*adapted from Levenspiel [13]*)

The solid reactant is initially surrounded by a fluid film, through which mass transfer occurs between the solid particles and the bulk of the fluid. As the reaction proceeds, an inert layer forms around the un-reacted core.

Leaching can be visualized as occurring in five successive steps.

1. Fluid reactant A diffuses through the film surrounding the particle to the surface of the solid.
2. Fluid A penetrates and percolates through the blanket of ash to the surface of the un-reacted core.
3. Fluid A reacts with the solid at this interior surface.
4. Fluid products are transferred through the ash back to the exterior surface of the solid.
5. Fluid products disperse through the gas film back to the main body of the fluid.

Not all of these steps occur in every leaching process. There is also considerable variation in the resistances of the different steps. Therefore the step with the highest resistance is considered the one that controls the rate.

The situation in which the fluid film controls the reaction is illustrated in Figure 2.2. Here, there are no products at the surface. The difference of concentration of A in the fluid phase C_{Ag} and in the solid phase C_{As} is constant at all times during the reaction.

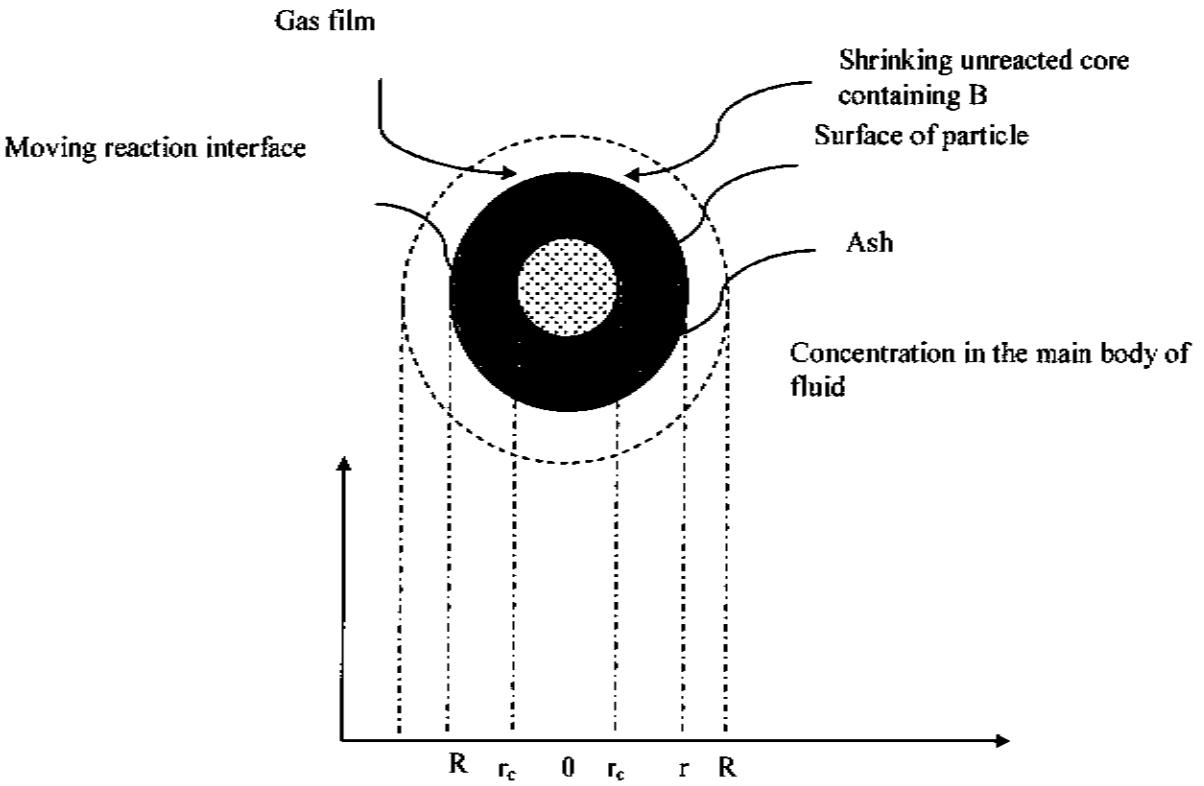

Figure 2.2- Representation of a reacting particle when diffusion through a gas film is the controlling resistance ***(adapted from Levenspiel [13])***

The flux of B is equal to the flux of A. Based on the stoichiometry of the reaction, this may be represented as:

$$dN_B = bdN_A \qquad (2.11),$$

Focusing attention on the unchanging surface exterior of the particle S_{ex}, we can write:

$$\frac{-1}{S_{ex}}\frac{dN_B}{dt} = \frac{-1}{4\pi R^2}\frac{dN_B}{dt} = \frac{-b}{4\pi R^2}\frac{dN_A}{dt} = bk_g(C_{Ag} - C_{As}) = bk_g C_{Ag}$$

=constant (2.12).

The amount of B present in the particle can be deduced by finding the product of the particle density ρ_B and the volume of the particle V:

$$N_B = V\rho_B \quad (2.13),$$

hence the decrease in radius of the un-reacted core that corresponds to the dissolution of dN_B moles of the solid reactant is:

$$dN_B = \rho_B dV = \rho_B d(4/3\,\pi r_c^3) = 4\pi\rho_B r_c^2 dr_c \quad (2.14),$$

Replacing equation 2.12 with 2.14 gives the rate of reaction in terms of the shrinking radius of the un-reacted core:

$$\frac{1}{S_{ex}}\frac{dN_B}{dt} = \rho_B\frac{r_c^2}{R^2}\frac{dr_c}{dt} = bk_g C_{Ag} \quad (2.15),$$

The integrating yields equation (2.15) that describes how the un-reacted core shrinks with time can be rearranged thus:

$$t = \frac{R\rho_B}{3bC_{Ag}k_g}\left[1-\left(\frac{r_c}{R}\right)^3\right] \qquad (2.16),$$

Assuming the time for the complete reaction of a particle is τ, at that time $r_c=0$, then:

$$\tau = \frac{R\rho_B}{3bC_{Ag}k_g} \qquad (2.17),$$

The radius of the un-reacted core in terms of fractional time for complete conversion is obtained by combining equations 2.16 and 2.17:

$$\frac{t}{\tau} = \left[1-\left(\frac{r_c}{R}\right)^3\right] \qquad (2.18),$$

thus, if:

$(1-x_B)$ = volume of un-reacted core /total volume of particle = $(r_c/R)^3$, the equation becomes:

$$\frac{t}{\tau} = \left[1-\left(\frac{r_c}{R}\right)^3\right] = x_B \qquad (2.19),$$

A similar analysis may be carried out for the cases when the rate-controlling step is the diffusion through ash layer controls or the chemical reaction. The corresponding rate equation for the different control regimes is presented in Table 1.

Table 1: Rate equations for different control regimes (*adapted from Levenspiel [13]*)

Control regime	Rate equation
Chemical reaction controlled	$\frac{t}{\tau} = 1-(1-x_B)^{1/3}$
Ash layer controlled	$\frac{t}{\tau} = 1+2(1-x_B)-3(1-x_B)^{2/3}$
Diffusion controlled	$\frac{t}{\tau} = x_B$

2.3.1.4 Using the shrinking core model

Because the shrinking core model has found widespread applicability in hydrometallurgical processes [18], we applied it when designing a prototype for integrated systems approach to the comminution and leaching processes . To provide a context for the different control regimes, a short outline of previous research is given here. Some researchers (Wen 1968) have commented on the unsuitability of the ash layer controlled regime to model hydrometallurgical processes. They suggest that this type of control regime is not suitable for modeling liquid solid reactions.

2.3.2 The Shrinking Particle Model

The shrinking particle model postulates that no ash layer is formed during the leaching reaction. The solid particles react with the liquid or gas reactant and shrink during the reaction, finally disappearing. The reactions are confined to the surface of the particle, the size of which is reduced by gasification and/or flaking of the solid products, as shown by equation 2.20.

$$A(g) + bB(solid) \longrightarrow \text{aqueous and solid products} \qquad (2.20),$$

Chemical reaction controls are similar to those exhibited by the shrinking core model. Deviation from the equation for diffusion controls is dependent on whether the particle is large or small. (See the equations summarized in Table 1.)

2.3.5 Selectivity of Leaching

Selectivity of leaching describes solubility of different metals during leaching. Many coarse-ore leaching processes involve the dissolution of one or more solid reactant from an inert porous matrix [8]. One of the metals will be of economic interest while the other may be unwanted. Selectivity should be such that the unwanted material is produced to its minimum, while the maximum amount of the metal of interest is leached

2.4 ATTAINABLE REGIONS ANALYSIS

Attainable regions (AR) analysis is a tool that was first introduced to optimize chemical reaction networks with complex kinetics. It was used to construct a configuration for a reactor system that would produce optimal results. The AR was defined in 1987 by Glasser et al. [9] as the set of all

possible outcomes that can be achieved for the system under consideration using the fundamental processes operating within the system, and which satisfies all constraints placed on the system.

2.4.1 Background of Attainable Region Analysis

In 1964 Horn [11] devised the AR as a way of representing all the possible states that can be reached by a reacting system, given a number of fundamental processes and parameters that can be controlled. Horn noted that it is possible to find the set of all possible output concentrations from all possible reactor systems for given kinetics and feeds. He called this set of possible outputs attainable regions, and postulated that if the AR is known, one can search the region to find the output conditions most appropriate to a given objective function, such as selectivity or maximum concentration.

The AR approach has two important uses when the process engineer is devising a system that will yield the best possible results. Firstly, searching for the maximum efficiency of an objective function over a defined set is fairly simple and straightforward. Secondly, the value of that objective function could also be used as a yardstick for comparative purposes. However, this conceptual tool was not applied in practice because Horn and others who subsequently followed up on his research were unable to find a systematic method of identifying the AR. Consequently, the AR method was not used for about 20 years.

Dyson et al. [7] located the AR by using optimization techniques to determine its boundaries. This method required that a family of optimization problems, rather than a single problem, should be solved, rendering the whole process complicated and offering little advantage in terms

of solving the difficulties raised by Horn's concept. However, when Glasser and Hildebrandt [10] re-examined the AR approach in 1987, they proposed the use of geometry to generate the AR boundary and region. They considered the fundamental physical processes that were taking place rather than concentrating on the individual pieces of equipment. In a simple homogeneous reactor, the fundamental processes are reaction and mixing. The AR could thus be constructed by developing an algorithm. Once all the possible outcomes for a system had been determined, it functions, for example cost or particle size distribution. AR analysis could thus be used to arrive at feasible regions of achievable states.

Interest in the application of AR analysis has grown over the last two decades. Although AR tool was first introduced to optimize chemical reaction networks with complex kinetics, the methodology has been extended to comminution processes, owing to the similarities between comminution and chemical reactions. Work done by Khumalo *et al.* [12] has suggested that AR based on the population balance model of comminution can be used to perform simultaneous process synthesis and optimization for a desired size class. In the project described in this dissertation, AR was applied to an integrated comminution and leaching system.

2.4.2 Procedure for AR analysis

2.4.2.1 Problem definition

A) Choose the fundamental process

Any physical process that may occur may be called fundamental. Typical examples in chemical engineering include reaction, mixing, heat transfer and mass transfer.

B) Select the state variables

These are variables that characterize the output state of the system. Those that sufficiently describe the rates of all the fundamental processes, the kinetics and the objective function that is to be optimized, and also obey the mixing rule should be chosen. Typically these could include concentration, mass fractions, reaction conversion and temperature.

C) Define the fundamental process vectors

Each of the fundamental processes, represented in the state space by a vector, is defined in such a way that there is an instantaneous change in the state of the variables in the system, if the fundamental process occurs. If we assume that the reaction is the fundamental process, the reaction vector r(c) defined at c represents the instantaneous change in c only if the reaction occurs.

D) The necessary conditions

The necessary conditions for AR are:

a) The region includes all the feed points.

b) No process vectors on the boundary of the region point out of the region.

c) No stationary point with mixing as a process exists in the compliment of the region.

2.4.2.2 Construct the region

An algorithm is developed and used to construct a candidate for the AR. Once a region is defined by a boundary that is proposed as a candidate AR, that boundary is tested in terms of the necessary conditions. Where the candidate is not completely correct and fails to satisfy one of the necessary conditions in some sections, an extension of the candidate region may be applied. The procedure is repeated until all the necessary conditions are fulfilled.

2.4.2.3 Optimize the process

The final stage is to find the point in the AR at which the process is optimized. In the majority of cases this occurs at a point on the boundary of the AR. (The boundary points represent the extremes of the process.)

2.5 INTEGRATED PROCESSES

Bade et al [3] developed a model to combine leaching and Comminution processes particularly for the analysis of the behavior of material in a reaction mill. Hence combining leaching and comminution processes is not a new phenomenon but has been used in trying to understand the reaction mill.

Over the last decade or so, mine operators have been under heavy pressure to reduce costs, as the price of supplies and services continues on an upward trend while commodity prices have fluctuated. This has prompted the idea of looking at both comminution and leaching as an integrated system as a means of cutting costs. The rationale behind this is that optimizing either the comminution process or the leaching process independently does not necessarily lead to optimum solution for the combined comminution-leach system Hence one has to look at optimizing the overall system and from this determine the operating conditions of the leach and comminution processes that will lead overall to the optimal operation of the system. Typically experimental data for the comminution process is fitted to comminution models, and experimental leaching data is fitted to leaching models. Currently flow sheets are developed by experience and the flow sheet optimized using simulations. However the question arises; was the chosen flow sheet the correct flow sheet? The goal of process synthesis is the identification of the best flowsheet structure that can carry out a particular task, such as conversion of a raw

material to product, in this particular case dissolution of minerals into solution. In order to accomplish this various approaches to process synthesis can be used some, of these include total enumeration that is limited to problems with reduced number of alternatives, graphical methods through physical insights or using heuristic evolutionary searches [6].

In this work we will look at using the AR approach to try to develop optimal flow sheets for simple comminution- leach systems.

2.6 COST ANALYSIS

The comminution and leaching process have cost implications attached to them. The comminution process is governed by the power law which is described in section 2.2.1. The third law of comminution states the energy of comminution is inversely proportional to the square root of the diameter of the product particles and is represented by the equation below:

$$E_b = K_b\left[\frac{10}{x_p^{0.5}} - \frac{10}{x_f^{0.5}}\right]$$

Where K_b is the bond proportionality constant.

The energy of comminution contributes to the bulk of the operation costs of the comminution circuit [12] The power law shows that the particle size and the cost of operation have a non linear relationship. As the particles become finer the cost of comminution increases, however since the relationship is non linear when the particles become finer and finer the cost of operation increases to a greater extent, as shown in figure 2.3. The rise in the cost of operation increases greatly as one tries to grind material to make it finer, this is shown in the plot, and the curve

becomes steep as the particles become smaller. Cost of comminution is mainly affected by the operational expenses (OPEX) i.e. the energy cost.

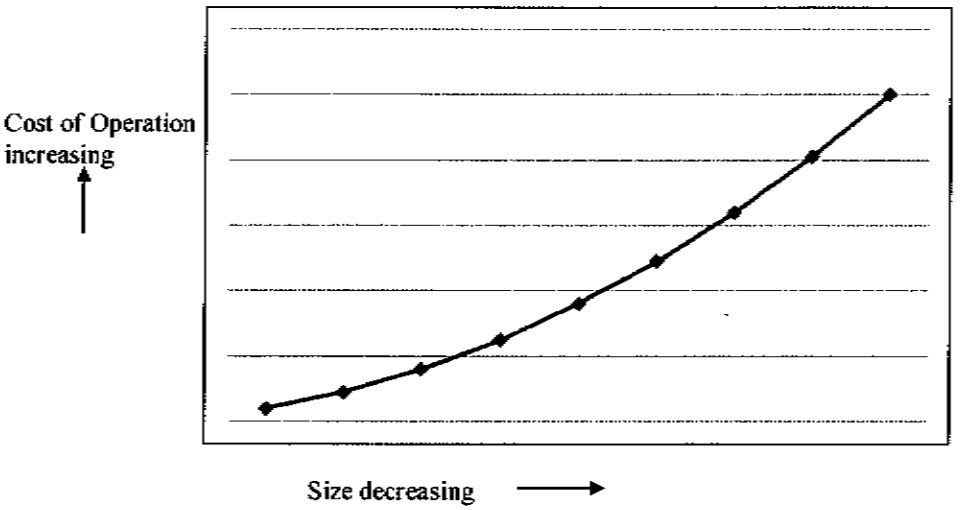

Figure 2.3: Sketch of Operating Costs based on the Comminution Process

The leaching process on the other hand is affected by the capital cost. The reaction time of the leaching process links to the residence time which will affect the size of the leaching reactor. The particle sizes have a direct effect on the reaction time and thus the residence time and ultimately the size of the leaching reactor. The size of the leaching reactor that the design calculations predict gives the designer an indication of the number of reactors that will be in the leaching cascade. Therefore the particle sizes predict the number of reactors that are needed in the leaching cascade. Finer size particles leach faster as predicted by the shrinking core model therefore will require less residence time and hence less amount of reactors. This has a direct effect on the capital expenses (CAPEX) of the leaching process. As the particle size decreases the expected capital costs is less as compared to the capital costs of the equivalent batch size with the larger particle size distribution.

This has a direct effect on the capital expenses (CAPEX) of the leaching process. As depicted in Figure 2.4 as the particle size decreases the expected capital costs is lower as compared to the capital costs of the equivalent batch size with a larger particle size distribution.

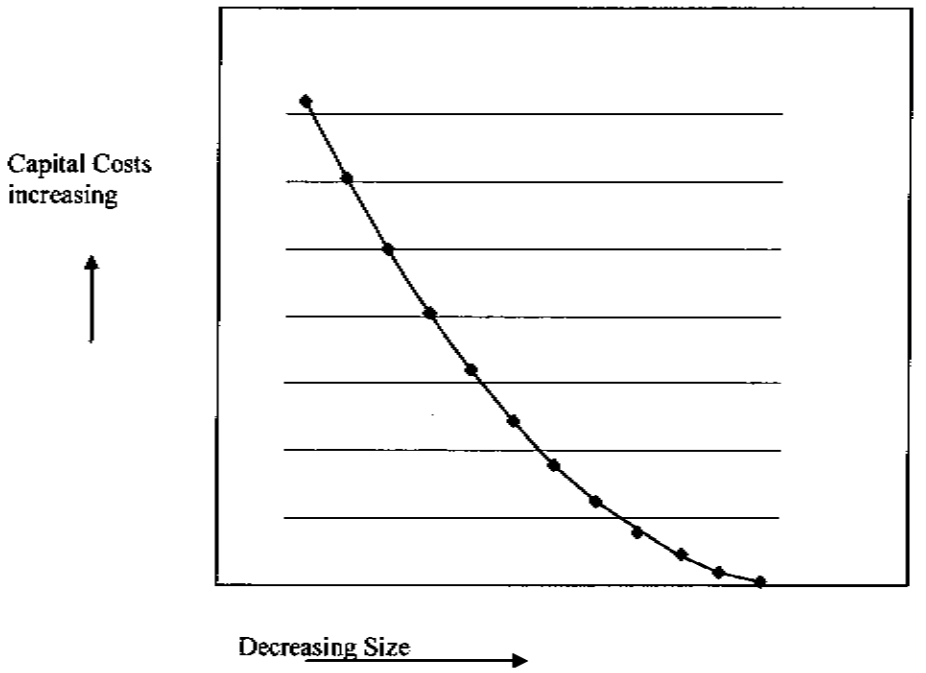

Figure 2.4: Sketch of Capital Costs based on the Leaching Process

The combination of figure 2.3 and 2.4, considers the leaching and comminution processes as an integrated unit. The integrated processes allows for an analysis of the CAPEX and OPEX of the overall processing plant. Considering the leaching and comminution processes as an integrated unit implies that there is a tradeoff between the benefit derived from less capital expenses

associated with finer particles in the leaching cascade which are accompanied by high operating expenses in the comminution circuit, compared with higher capital expenses associated with larger particles in the leaching cascade which are accompanied by lower operating expenses in the comminution circuit. Integrating the leaching and comminution processes allows for an analysis of the CAPEX and OPEX and hence giving an opportunity for optimization of the processes.

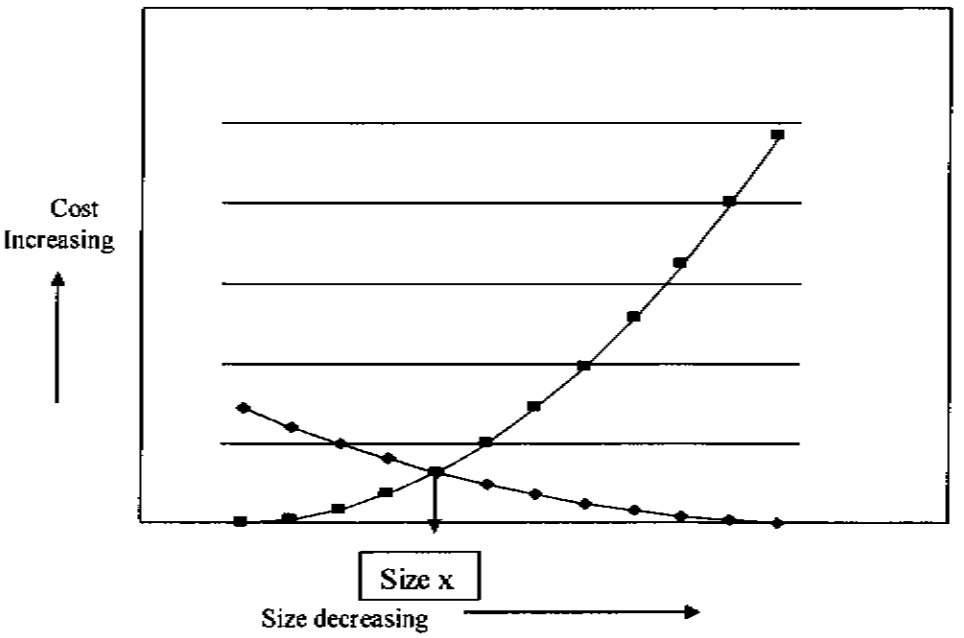

Figure 2.5: Combined CAPEX and OPEX plot

Figure 2.5 shows the curves for the particle CAPEX and OPEX; they cross at particle size class (x) which is the optimal size of operation when considering major costs associated with the two processes.

Energy costs are critical particularly in South Africa, where the electricity supplier for the nation is facing great challenges in providing adequate electricity to the nation. Most of the energy consumption is attributed to the various industries in the country. Comminution is one of the industrial processes in South Africa and innovative ways of improving the energy efficiency of the process can contribute to the reduction in the strain that the energy provider (ESKOM) is facing.

CHAPTER THREE – MODEL OF THE INTEGRATED COMMINUTION-LEACH SYSTEM

3.1 INTRODUCTION

Modeling is an important tool used in the understanding of processes. Complex mechanistic models are used in the study and optimization of heterogeneous mineral processing of particulate systems. Process engineers are increasingly required to achieve deeper insight into processes in order to optimize process designs and achieve effective process synthesis. Only the intelligent use of well understood relationships and properties will lead to optimized design and processing solutions. Mathematical modeling of fluid-solid systems is usually used to interpret experimental results as well as to gain insight into the reaction mechanisms in leaching systems.

The operational costs of leaching and comminution are affected by a variety of factors including energy usage during comminution; lixiviate consumption during leaching, time of operation etc. Generally the objective functions considered in such systems are those which would give the optimal particle size distributions for the leaching process, thus ultimately positively affecting the cost of these particular unit operations. The grinding process energy efficiency is in the range 4-8% accessed on the basis of surface area produced [12]. This implies that the process of comminution has a great deal of wastage of energy. Comminution of minerals independent of the downstream processes can lead to over-grinding of material. As discussed above, the process of comminution is energy intensive; any additional energy used in the comminution process which does not positively affect the downstream process is a waste. The comminution process is thus inefficient as a unit operation based on the grinding process efficiency stated above as well as based on the fact that it may not directly address the target of the downstream process.

Since it is the ultimate objective to produce minerals of a specified purity at the lowest possible cost, it is proposed that the attainable region analysis potentially offers the opportunity to optimally combine the fundamental processes occurring in comminution and leaching, thereby hopefully maximizing the final product or minimizing the cost of the processes. A more efficient process has the potential of enhancing the profitability of the relevant industries.

3.2 INTEGRATED GRINDING AND LEACHING PLOTS

The researcher proposes a system in which the comminution and the leaching processes are considered as batch operations as depicted in Figure 3.1.

In this study we consider only three size classes namely; the feed size - Class 1, the median size - Class 2, and the fines size - Class 3 in order to be able to graphically represent the comminution. Consider the following thought experiment: Feed of size class x_1 is loaded into a batch comminution process. Comminution occurs for a given time (t). No material is added to or taken away from the system once the batch comminutes. For ease of representation we imagine the breakage process as occurring in one unit representing a series of breakage events which yield a variety of mass size classes. This approach is general and can be expanded to any number of size classes The thought experiment continues as follows: The material ground for a time (t_g) in the batch mill is then charged into a batch leaching reactor where it undergoes leaching for a further time interval t_l. Each size class is subject to varying leaching rates due mainly to the different radii of the particles. We assume initially that only the mineral of interest goes into solution. This constraint will be lifted in later examples

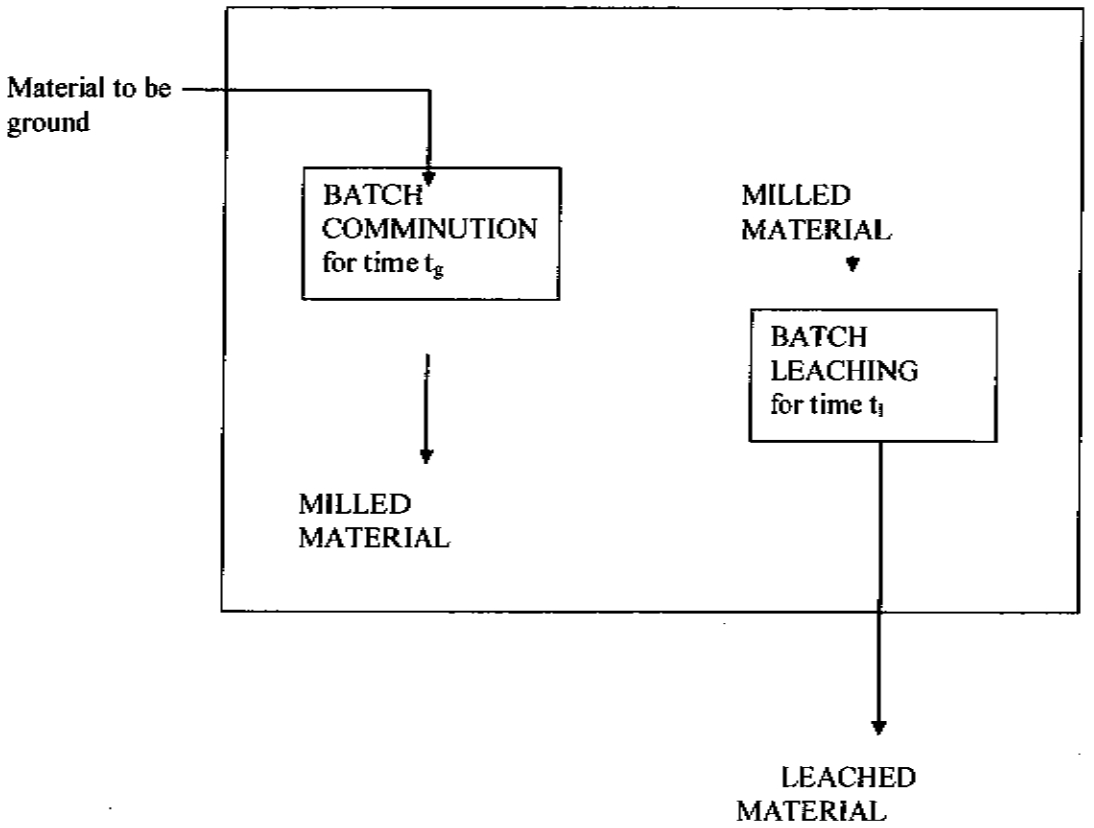

Figure 3.1 – Schematic view of the batch comminution- leaching system

3.3 BATCH SIMULATION OF MILLING

The comminution and leaching processes were modeled using the Matlab® Simulation software package with the algorithm developed for this study given in the appendix. Comminution can be considered as a first order rate process. The population balance model outlined in section 2.2.2 was used to predict comminution behavior. The model takes into account all sub processes of breakage kinetics, material transport and size classification. The Matlab algorithm used equations 2.7, 2.8 and 2.9 to model the comminution process

Table 2: Breakage and selective function for classes 1 and 2

	Class 1	Class 2
Selectivity Function (s) per unit of time	1	0.5
Breakage Function (b_{21})		0.5

Table 2 above shows the values of the breakage function and the selective function used in this work. Assuming a feed of material containing 100% of size class 1 particles is charged into the batch comminution circuit and comminution is allowed to proceed for a specific unit of time t_g which can be seconds, minutes or hours depending on the type of material or the quantity of material being ground. The simulation of the comminution process yields size class fraction depicted in Figure 3.2. The mass distributions of size class one shows an exponential decrease. The median size (size class 2) runs to a maximum and then starts to decrease as comminution progresses. The mass fraction of Size class 3 particles increases as time progresses approaching 1 at time $\rightarrow \infty$.

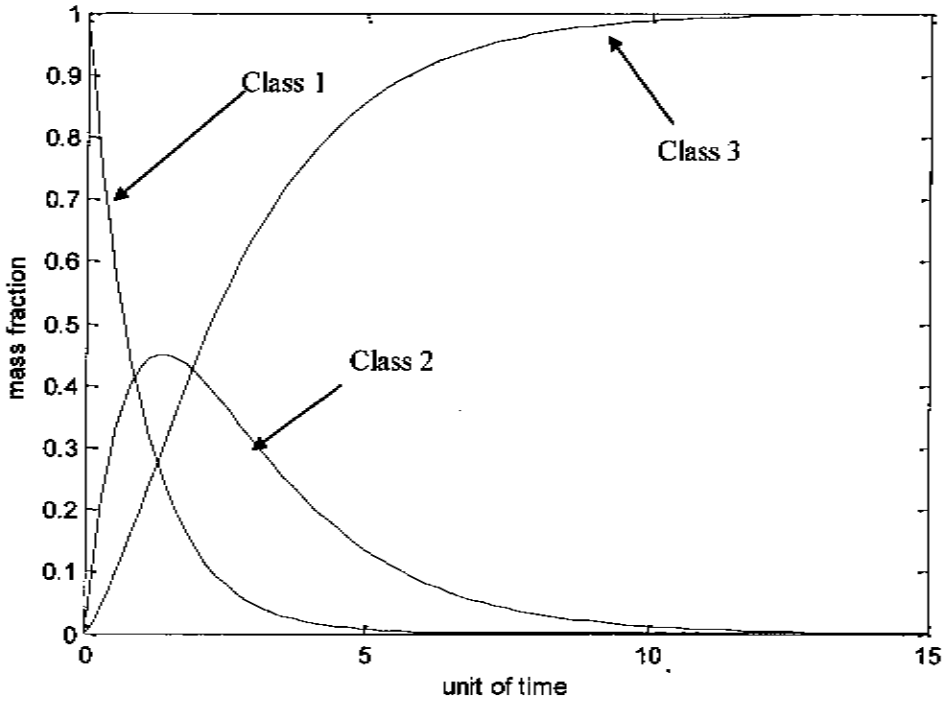

Figure 3.2 – Simulation of the particle size distribution after batch comminution as a function of grinding time

The batch leaching process is directly related to a continuous mill if the solids flow in plug flow along the mill and the energy intensity of the interaction between the balls and the solid is kept the same as in the batch mill. In this case the unit of time of the x axis in Figure 3.3 would be interpreted as residence time in the continuous plug flow mill. We see that there are opportunities to change the product size distribution by running mills in parallel.

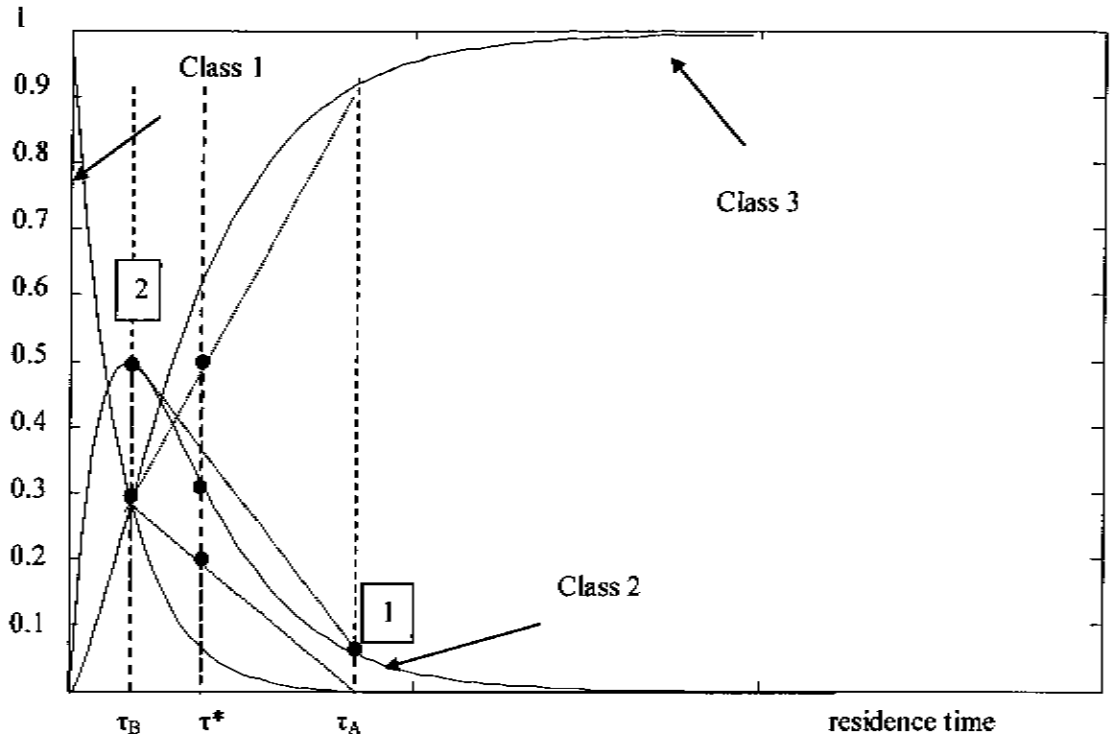

Figure 3.3 – Simulation of the particle size distribution after batch comminution as a function of grinding time

For example: Consider the following configuration in the milling circuit:

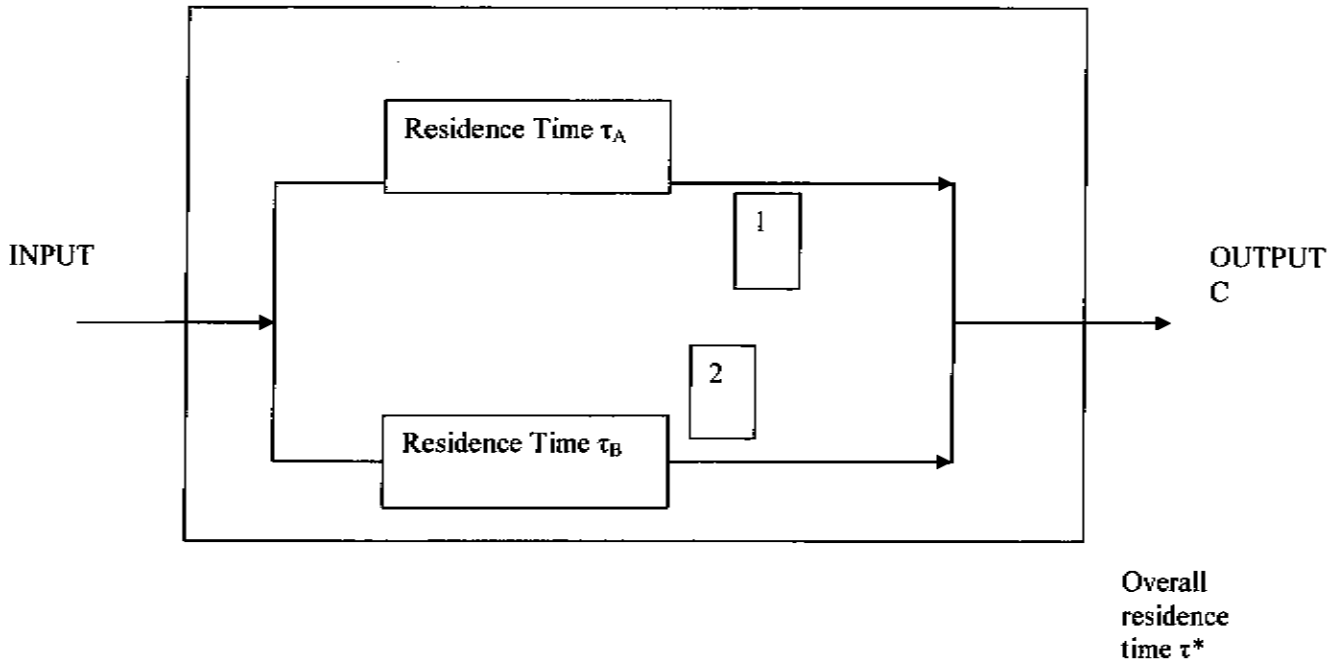

Figure 3.4 – Parallel configuration of a milling circuit

If we could run one mill with a residence time τ_A then the output (1) would be as shown in fig 3.3 at point 1. Similarly we could run the mill with residence time τ_B which would, as can be seen in fig 3.3 have less grinding occurring with more material in size class 1 as shown in at point 2. If we run these two mills in parallel and mix the streams, we could achieve the product distributions represented by the dotted line between 1 and 2. Thus depending on the relative mass flows through the 2 mills, one could achieve any point along the line.

Suppose we set the mass flows so that the mass flows through the mill A is M_1 and that through mill B is M_2. The overall residence time of the mill system (i.e. if the 2 mills are in parallel) is τ^* so that: $(M_1+M_2)\,\tau^* = M_1\,\tau_A + M_2\,\tau_B$

Suppose τ^* is as shown in figure 3.3. We see that the parallel mill system would achieve mass fraction of size class 1 of 0.07, size class 2 of 0.30, size 3 of 0.63 as shown in figure 3.2. In contrast a single mill running at a residence time of τ^* would achieve mass fraction of size class 2 of 0.35 as shown in figure 3.2. Hence if we wished to produce more of size class 2 and less fines, the parallel mill would do better than a single mill with the same residence time. *We thus see there are opportunities to modify and optimize the mill output depending on the structure of the system that is used.* This was investigated by Khumalo et al [12] and the type of approach used above comes from the attainable regions concepts.

3.4 THE INTEGRATED BATCH LEACHING AND COMMINUTION SYSTEM

The leaching processes were modeled using the Matlab® Simulation software package with the algorithm developed for this study given in the appendix. Following the thought experiment, the material in the comminution process is charged into the leaching reactor. At a certain time t, material from the comminution circuit is charged into the leach reactor and undergoes leaching to completion. The grinding time was set at a value t_g which determined the size distribution of the material leaving the batch comminution process. The material with this size distribution was then used at a feed to the simulation of batch leaching process and the resulting dissolution was calculated. The grinding time t_g was varied in the simulations and the times used as well as the corresponding product size distributions from the batch milling process are listed in Table 3 and are also shown graphically in figure 3.5. Different grinding times have different distributions of particles in size class1, 2 and 3 hence the feed distribution to the leach system changes which

affects the resulting dissolution. The sum of the leached mass is then modeled to get the resultant leach curve at any particular leaching time t_l.

Table 3: Grinding times t_g and associated size distributions from the mill. These materials were then used as feeds for the leach process simulation.

Sampling time	Unit of time	Size Class1	Size Class 2	Size Class 3
t_0	0	1.0000	0	0
t_1	0.1395	0.8698	0.1131	0.0171
t_2	0.8270	0.4373	0.4032	0.1595
t_3	1.4578	0.2327	0.4495	0.317
t_4	3.3531	0.0350	0.2737	0.6914
t_5	5.3191	0.0049	0.1171	0.8780
t_6	7.2850	0.0070	0.0459	0.9534
t_7	9.4060	0.0001	0.0162	0.9837
t_8	12.4846	0	0.0035	0.9965
t_9	16.4650	0	0.0005	0.9995
t_{10}	20.9388	0	0	1

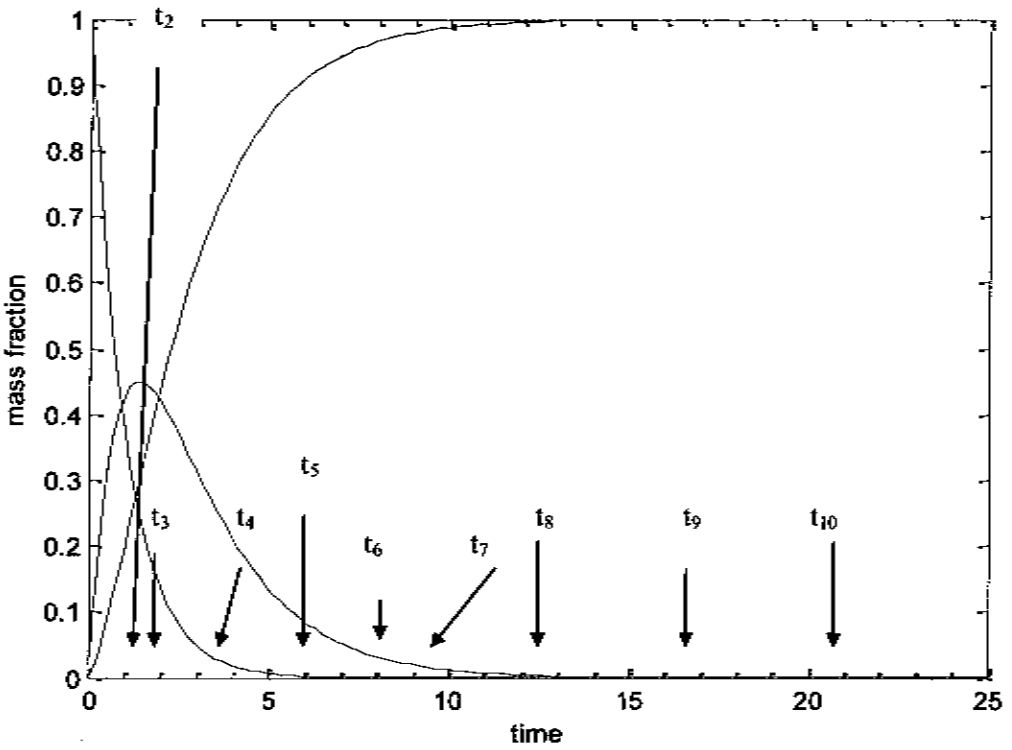

Figure 3.5 – Simulation of the particle size distribution after comminution as a function of grinding time t_g. The grinding times used in the simulations are shown. These grinding products were used as feeds for the leach process simulations.

For the shrinking core model where the chemical reaction is controlling the leaching, Table 1 in Chapter 2 shows that:

$$\tau \propto R$$

Simulations were carried out using the *chemical reaction control* model to determine the conversion of the solid for each size class. The reaction time for complete conversion τ is initially chosen so that the leaching is slow compared to the time constants of grinding. Table 4 gives the assumed times for complete conversion of the three particle size classes for the chemical reaction controls.

Table 4 – Specified Times for Complete Conversion for Particle Size Classes for the Chemical Reaction Control

Particle Size	Reaction Time (unit of time)
1	500
2	200
3	100

Table 5 shows the color code for the different leach curves.

Table 5 – Color Codes for curves

Sampling Times	**Color of curve**
t_0	Black
t_1	Dashed Blue
t_2	Yellow
t_3	Magenta
t_4	Cyan
t_5	Solid Blue
t_6	Green
t_7	Red
t_8	Blue Dash and Dot
t_9	Black
t_{10}	Blue Dot

Figure 3.4 shows the leach results at $t_g = t_0 = 0$; in this case the feed material to leach has not been subjected to any form of grinding therefore contains only particles in the feed size (class 1).

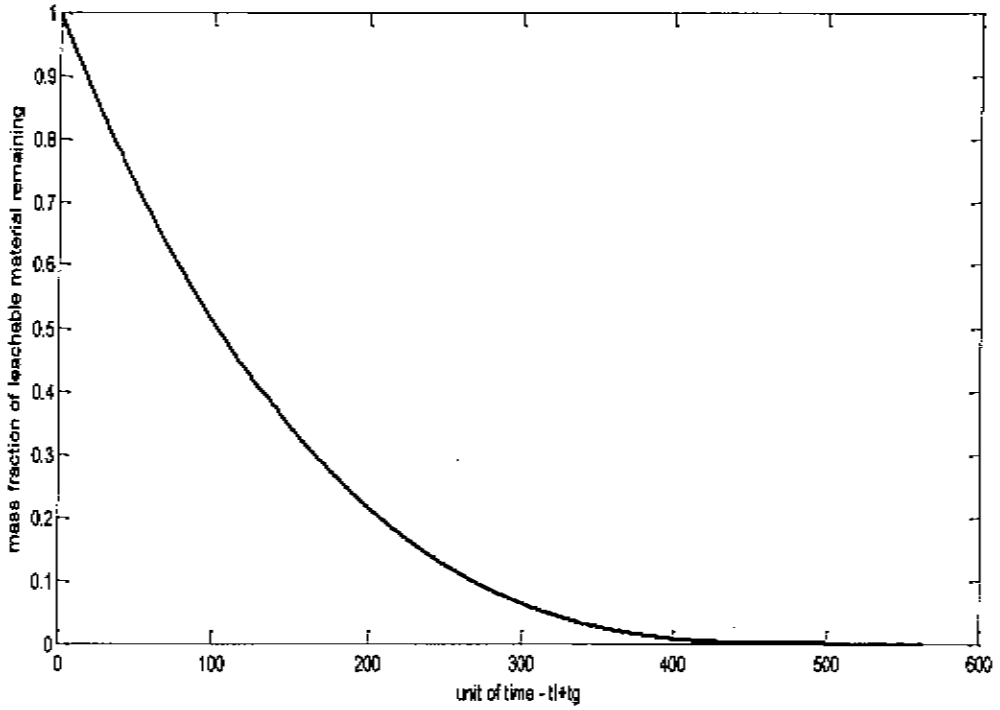

Figure 3.6–Simulated leach curve for chemical reaction control. The initial mass fraction corresponds to the mass fraction of that size class in the stream from a comminution process at time t_0 as defined in Table 3 – corresponding to material that has not been ground and which therefore consists of size class 1 only.

Figure 3.6 shows that there is a decrease in the mass fraction of leachable material as the time of leaching progresses and it approaches 0 at 500 units of time.

At a grinding time of $t_g = t_1$ the feed material to the leach contains some particles in the other size classes because grinding has began. The mass fraction distribution at t_1 is given in table 3. In our

simple model of the leaching process, each particle size class is subjected to leaching independently of the other particle size classes in the system.

The leaching of each of the individual size classes as a function of leaching time t_l is shown in Figure 3.7. The slopes of the curves in Figure 3.7 differ due to the difference in the leaching rates of the different size classes. As can be seen from Table 1 in Chapter 2, the rate of leaching is proportional to τ which in turn is proportional to the size of the particle. The blue curve in Figure 3.7 represents the leach pattern of particles in size class 1, the red curve particles in class 2 and the black curve particles in class 3. For illustration purposes the ore is assumed to have 100% of the leachable material. The mass fraction of the particle size classes goes to zero at the corresponding reaction time τ for the size classes i.e. Class 1- 500 units of time, Class 2 – 200 units of time and Class3 – 100 units of time.

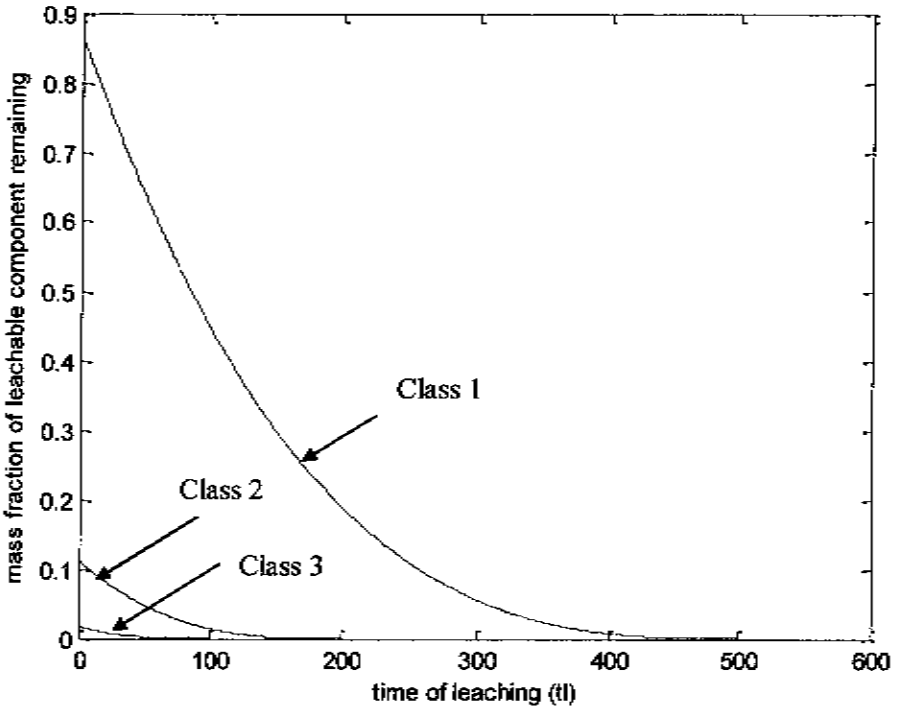

Figure 3.7 –Simulated leach curves as a function of leaching time t_l for chemical reaction controls. The initial mass fraction corresponds to the mass fraction of that size class in the stream from a comminution process simulated to run for time $t_g=t_1$ as defined in Table 3.

The resultant leach curve for this system (that is corresponding to a comminution time $t_g= t_1$ as shown in Table 3) is given in figure 3.8. This is obtained by adding the mass fraction of the leachable component remaining during the leaching process.

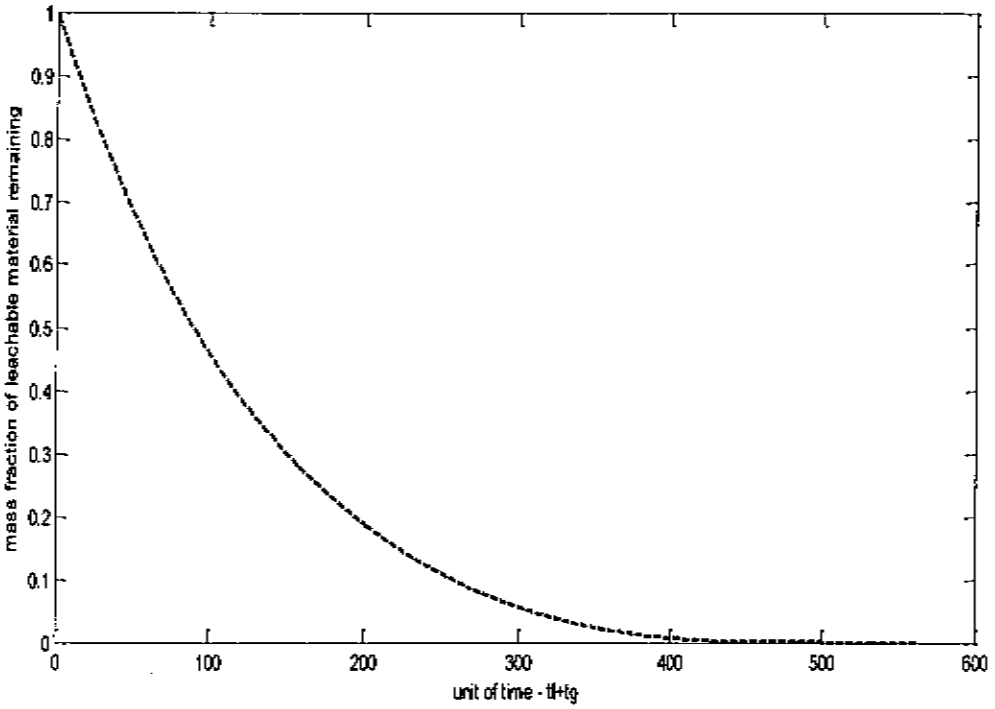

Figure 3.8 – The resultant leach curve. The feed to the leach is the material from the grinding process after the grinding process has run for time t_1 as defined in Table 3

The resultant curve is a summation of the individual leach curves for the 3 size classes, shown in figure 3.8. Each particle size class has an effect on the overall leaching kinetics of the process. Total dissolution of the material occurs after 500 unit of time. The graph shows that a significant proportion of material is leached by time of 400 units.

When the mill has run for time t_2, as define in Table 3, the proportions of particles in size class1, 2 and 3 have changed because grinding has occurred for a longer time. The resultant leach curve obtained is given in Figure 3.9

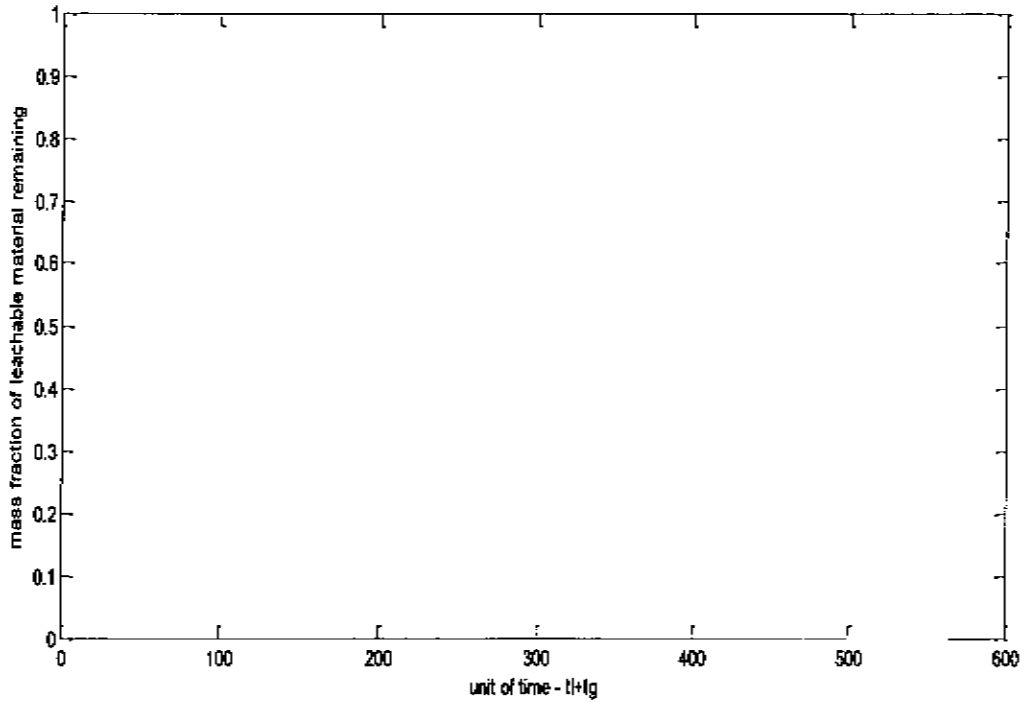

Figure 3.9 – The resultant leach curve. The feed to the leach is the material from the grinding process after the grinding process has run for time t_2 as define in Table 3

The graph shows that a significant proportion of material is leached by time of 380 units. This is in a shorter time than the scenario at t_1. This is due to the increased proportion of material in size class 3 which leaches faster than other classes. Figure 3.10 shows the leach curves at time t_2.

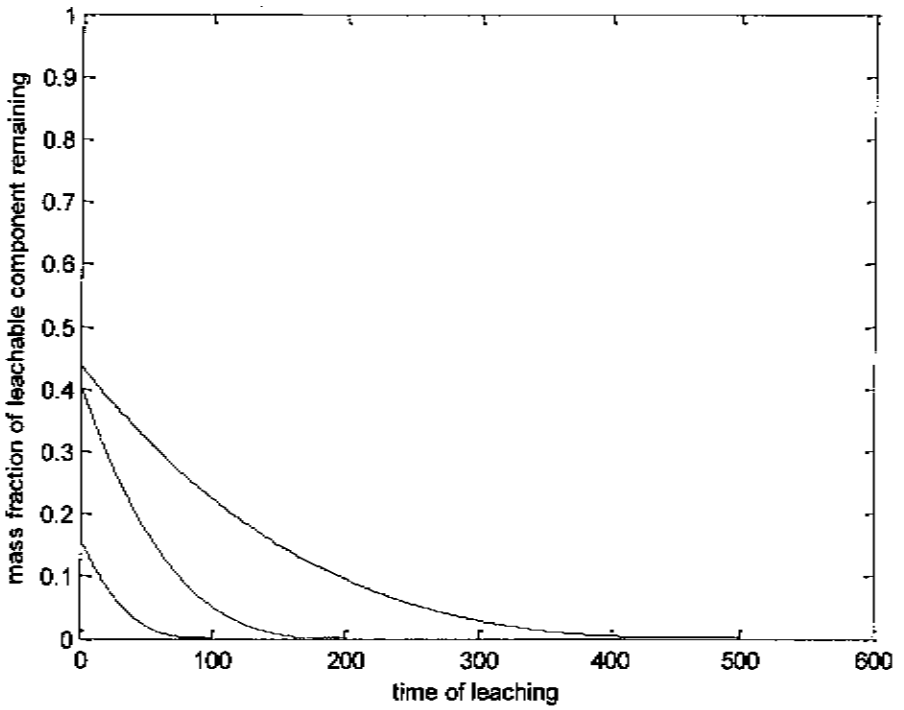

Figure 3.10 –Simulated leach curves for chemical reaction controls. The initial mass fraction corresponds to the mass fraction of that size class in the stream from a comminution process at time t_2 as defined in Table 3.

At t_3, the resultant curve is given in figure 3.11. There is an increase in the amount of material in size class 2 due to the breakage of particles from class 1 and an increase in material from class 3 due to a breakage from class 2 and 1. However due to the differences in proportion of the size classes 1,2 and 3 significant amount of material is leached out slower than for t_3=t_2

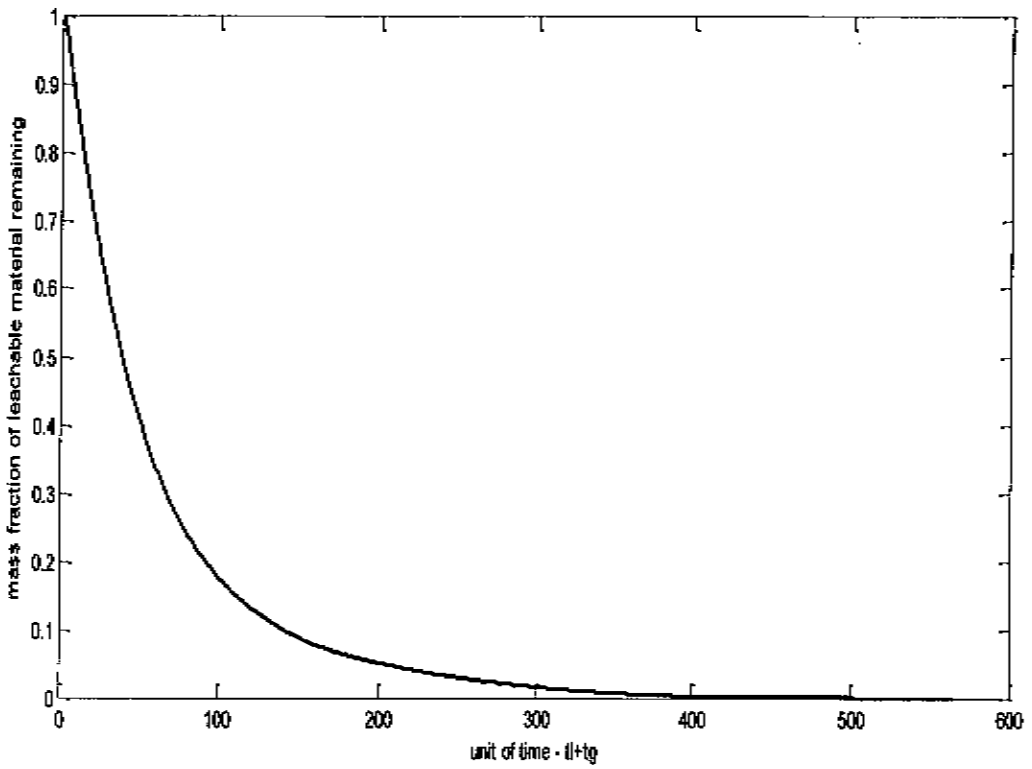

Figure 3.11 – The resultant leach curve. The feed to the leach is the material from the grinding process after the grinding process has run for time t_3 as define in Table 3.5

Figure 3.12 – Figure 3.18 shows the curves at t_4, t_5, t_6, t_7, t_8, t_9, and t_{10},. The series of graphs show that as the grinding time increases the resultant leaching will occur in a shorter time. At t_4 the quantity of material in the size class 2 begins to decrease. Material breaks out of class 1 to class 2 and class 3, in addition material in class 2 breaks out into class 3. Hence the quantity of material in size class 3 is increased greatly; the resultant leach curves show that the leaching occurs at a faster rate.

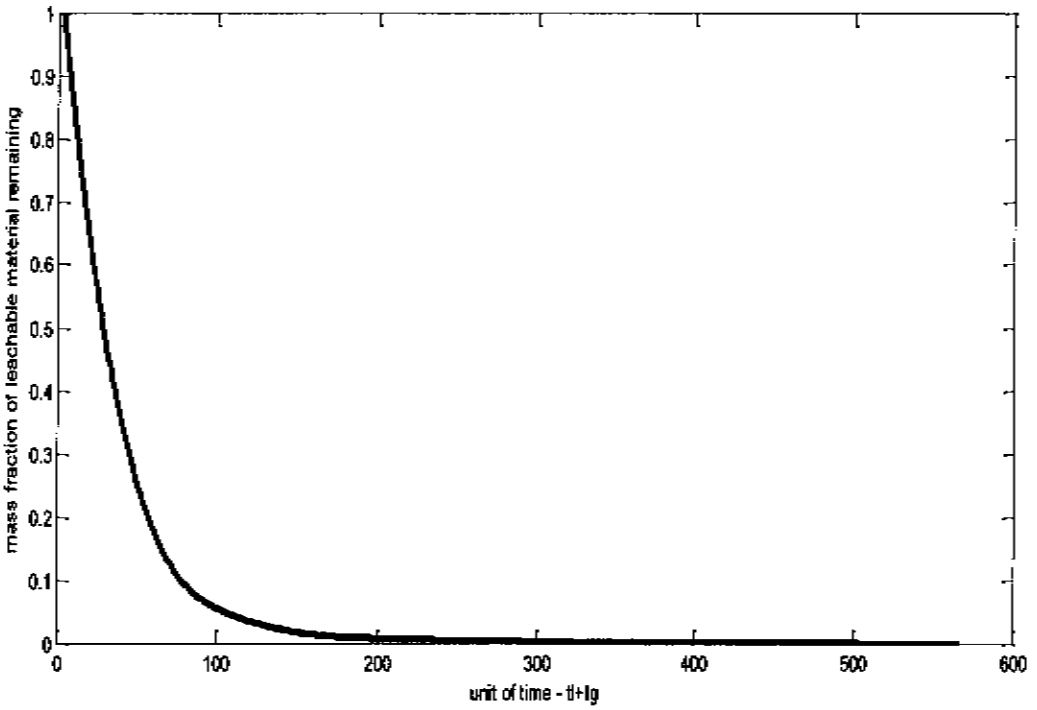

Figure 3.12 – The resultant leach curve. The feed to the leach is the material from the grinding process after the grinding process has run for time t_4 as define in Table 3.

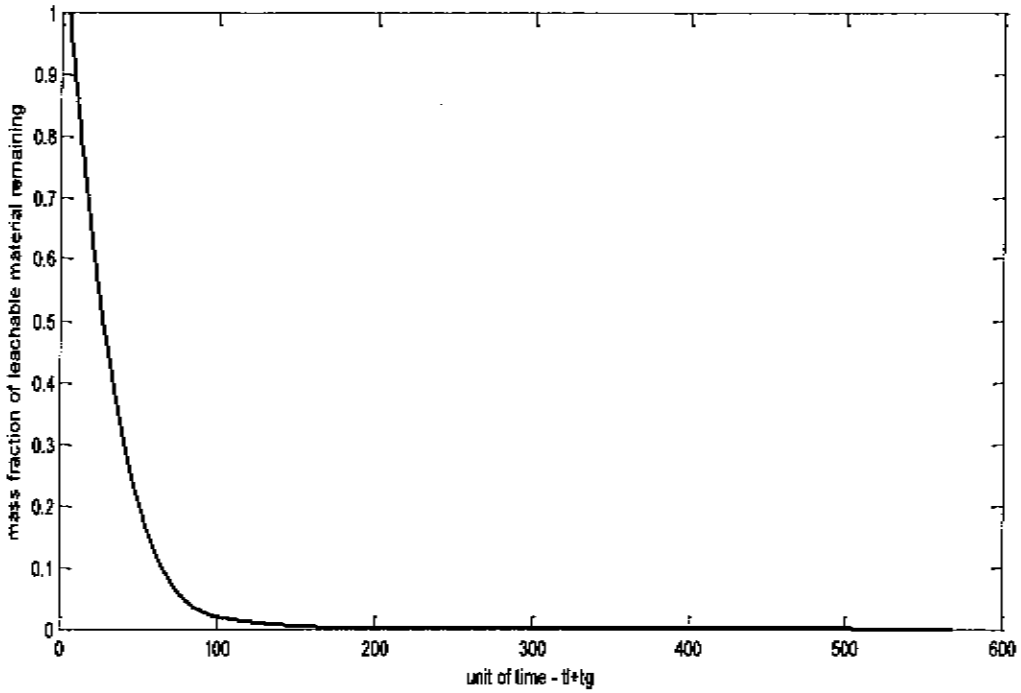

Figure 3.13 – The resultant leach curve. The feed to the leach is the material from the grinding process after the grinding process has run for time t_5 as define in Table 3

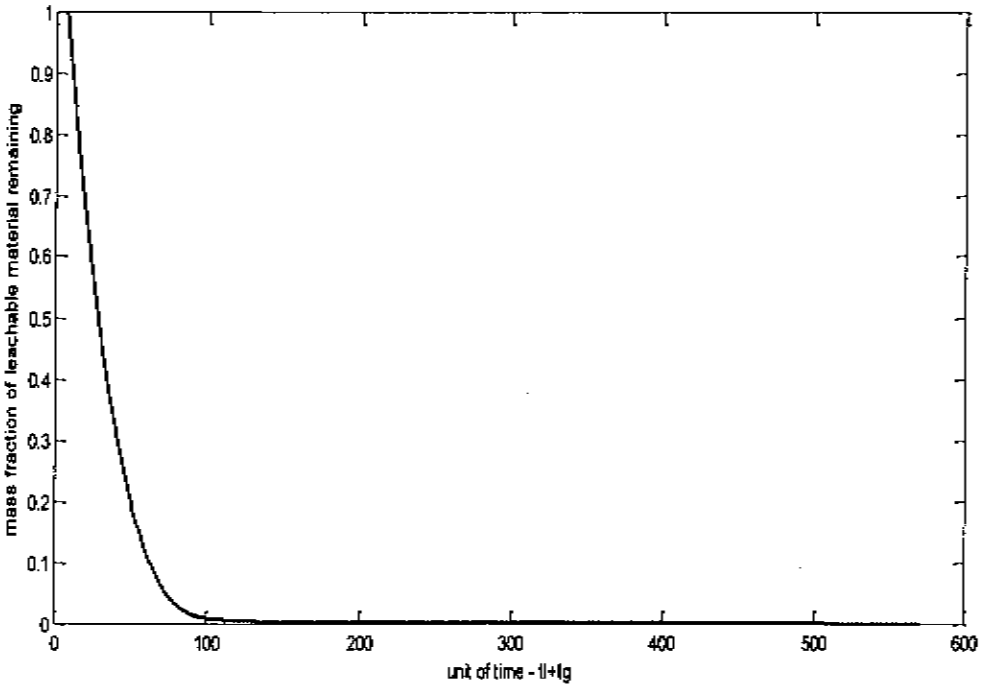

Figure 3.14– The resultant leach curve. The feed to the leach is the material from the grinding process after the grinding process has run for time t_6 as define in Table 3.

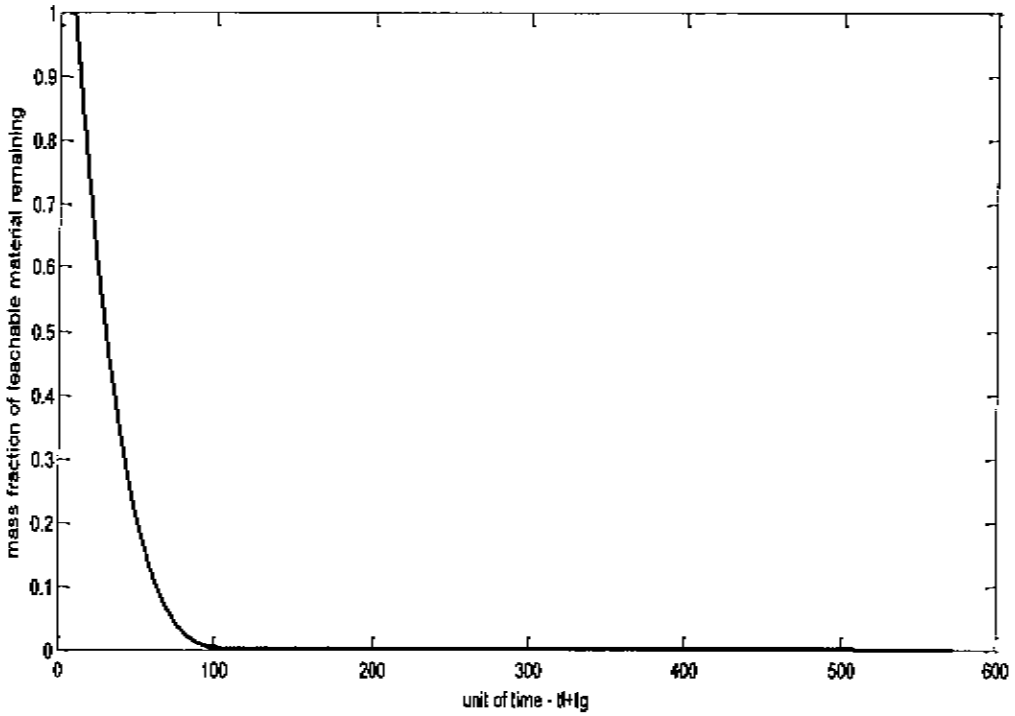

Figure 3.15 – The resultant leach curve. The feed to the leach is the material from the grinding process after the grinding process has run for time t_7 as define in Table 3.

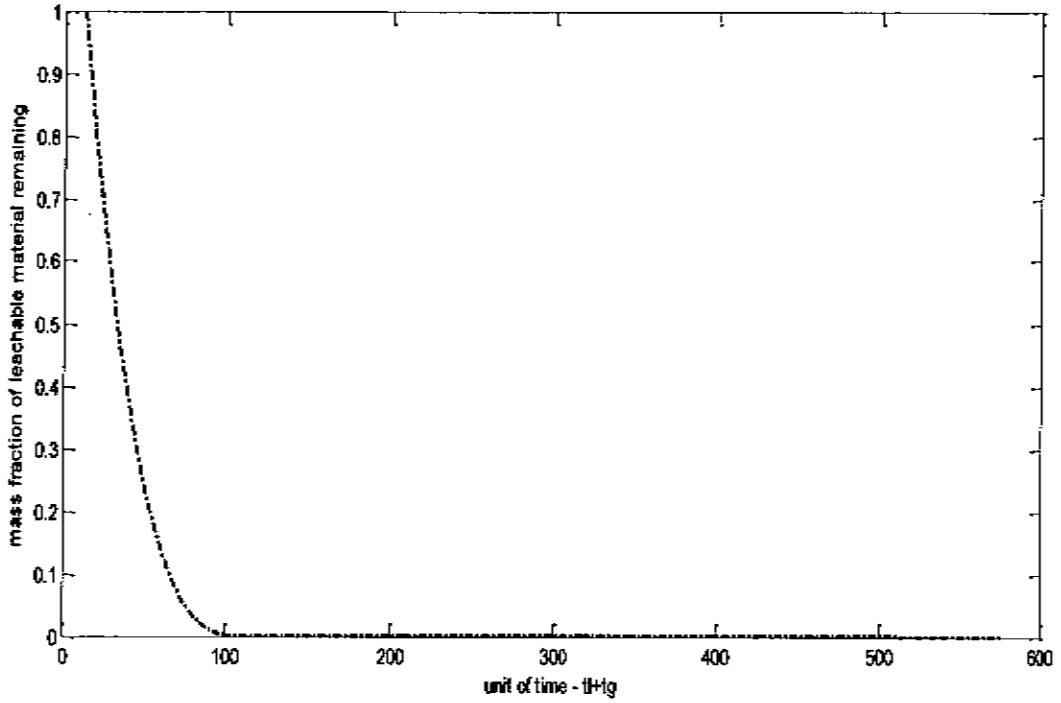

Figure 3.16 – The resultant leach curve. The feed to the leach is the material from the grinding process after the grinding process has run for time t_g as define in Table 3.

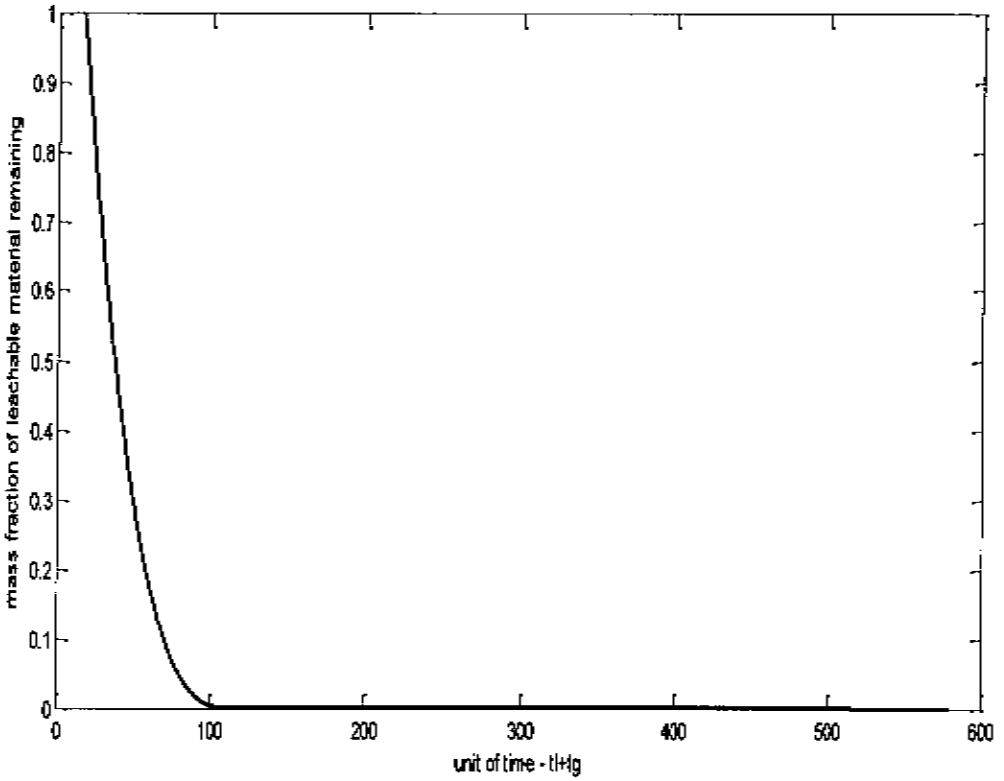

Figure 3.17 – The resultant leach curve. The feed to the leach is the material from the grinding process after the grinding process has run for time t_9 as define in Table 3.

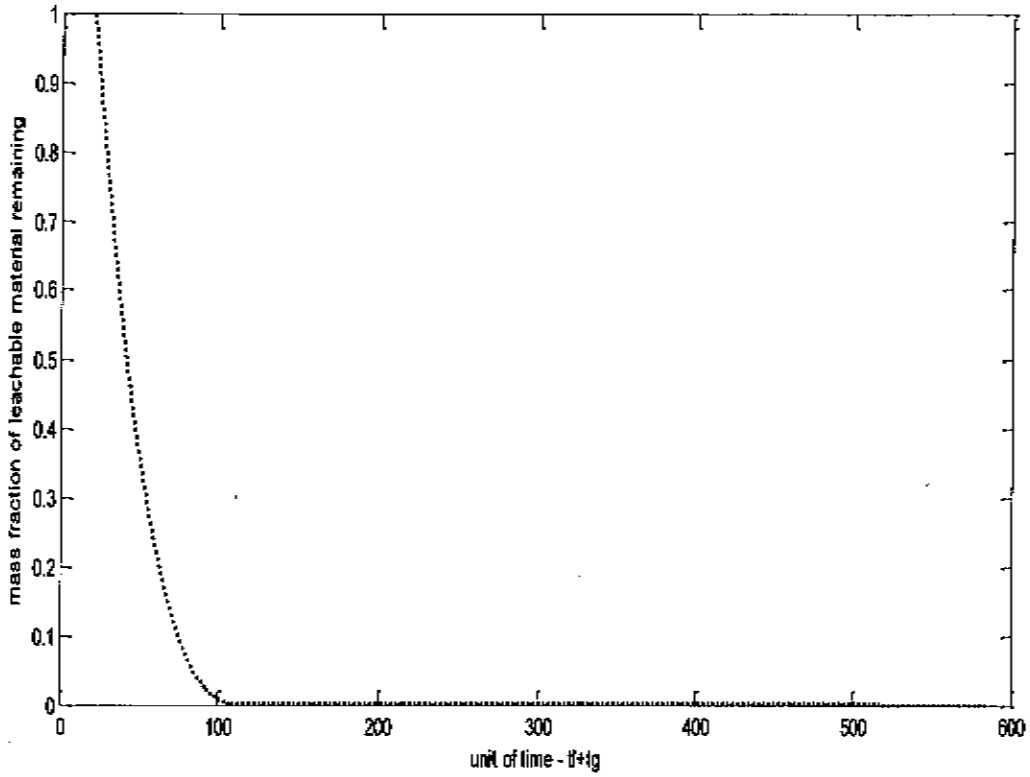

Figure 3.18 – The resultant leach curve. The feed to the leach is the material from the grinding process after the grinding process has run for time t_{10} as define in Table 3.

The slopes of the leach curves differ due to the difference in size of the particles. The leach curves from t_1 to t_{10} are shown in figure 3.19. Figure 3.19 is a combination of figures 3.18, 3.17, 3.16, 3.15, 3.14, 3.13, 3.12, 3.11 and 3.9. The corresponding time of leaching and grinding to the color of the curves given in Table 5.

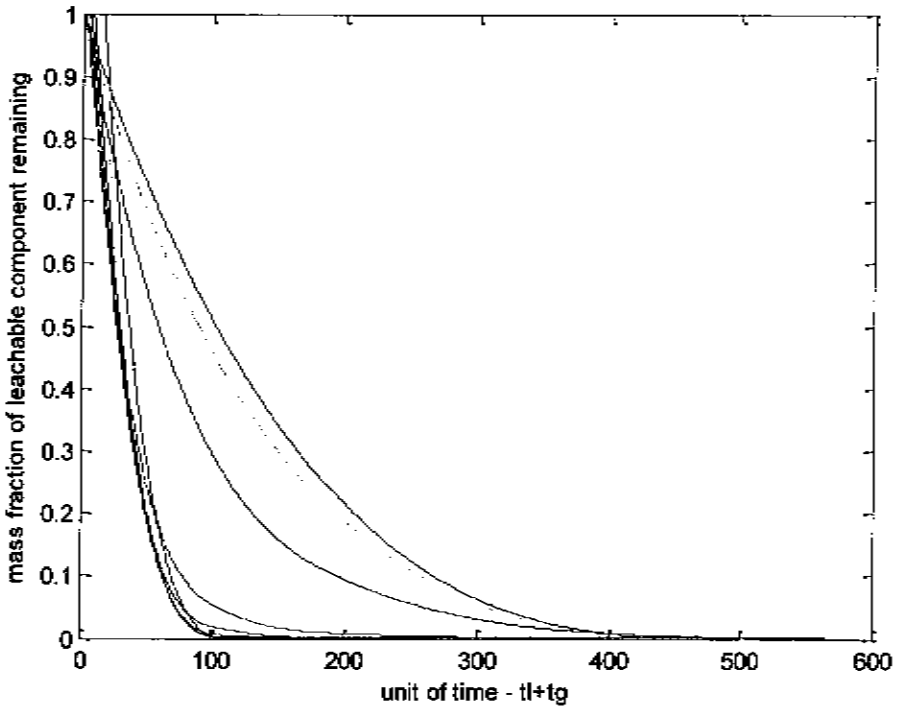

Figure 3.19 –Overall leaching curves as a function of combined grinding and leaching time, where the grinding time is varied from time from t_1 to t_{10}, as defined in Table 3.

As described in section 3.2, all the material from the comminution process is charged into the leaching reactor where it undergoes batch leaching. At leaching time t_{10} greater than t_1 the leaching curves generally become progressively steeper, due to the increase in the proportion of

the amount of material with particles of size class 3. The particles in size class 3 accelerate the conversion rate.

If we assume a target of 75% dissolution of the mineral ore is targeted and run the simulation accordingly, the results are shown in figure 3.20. Leach curves t_5 and t_6 which represent two different size distributions of leached material, reach the targeted dissolution rate at the same time. They however have varying proportions of size class 1, 2 and 3. The proportions of $m_1:m_2:m_3$ at t_5 are 0.005:0.117:0.878 respectively while, for t_6 are 0.000:0.0460:0.954 respectively, the leach times where 75% dissolution of material occurs is 46units. This shows that if a target of 75% dissolution is required the ore need not be milled to point to t_6, that will be a mere wastage of energy it will not give any added benefit to the leaching process. A similar deduction can be made, when other control regimes are being considered as shown in section 3.4.1; this model can be applied to any type of leach kinetics that the mineral is subjected to. Though it may be a well known fact in hydrometallurgy that leaching is a particulate reaction dependent on the distribution of size particles in the ore this model was developed to show how to predict how the distribution of the size classes directly affects the leaching as well as the comminution processes.

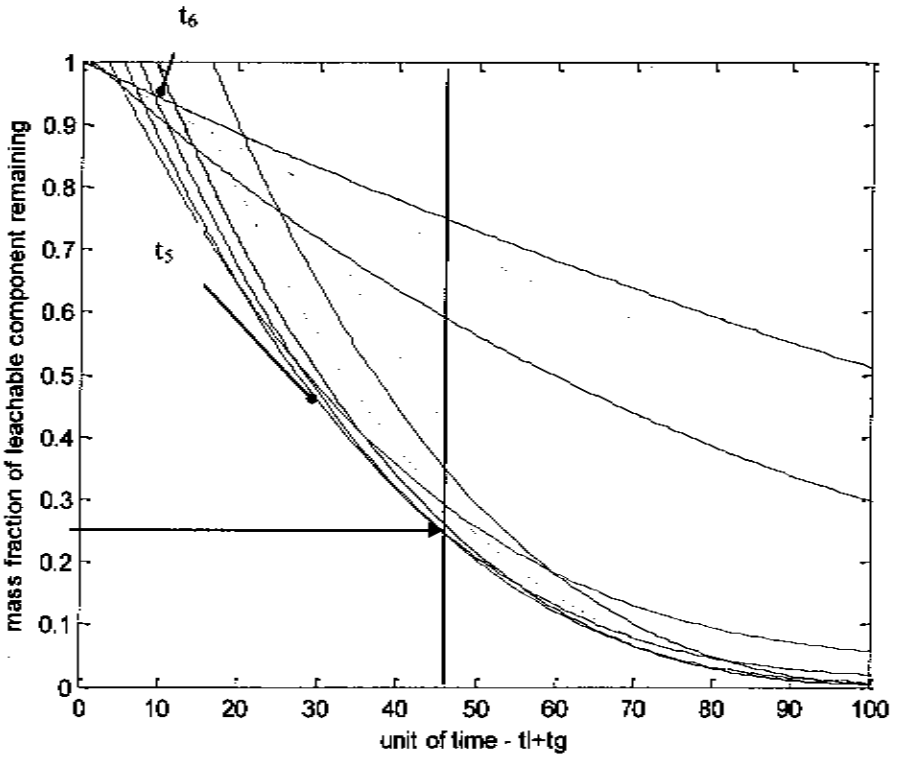

Figure 3.20- Magnified resultant leach curves

The derived integrated systems show that each size class contributes to the leaching regime, hence the varying proportions of material in each size class give use a leach curve. If we pose a scenario where the capacity of the mill is 200kg and when the comminution is done to full capacity and all material is fed to a corresponding size leaching tank. The integrated system shows that the comminution process can be done to full capacity; however the ground material can be fed to more than one leach tank. Some of the ground material is mixed with the unground material. This reduces the energy used in comminution because the comminution cycles are reduced whilst the amount of material leached remains constant.

Leaching, according to the model developed occurs at a faster rate for particles with a small radius, i.e. the particles in size class 3. Fines may become entrained with air and lead to a lot of

dust explosions and flow stoppages. Fines also stick to the process equipment, leading to the reduction of plant efficiency and increased downtime. The production of fines in the comminution process also leads to a phenomenon known as the cushioning effect which leads reduced efficiency of the comminution process. When one considers the leaching process in isolation, to increase leaching rate, one would feed the fines into the leaching system. However the integrated model shows that the feed from comminution to leaching contains particles of different sizes. The contribution of the size classes thus affects the leaching rate. Milling along time does not necessarily benefit the leaching process rather an intermediate time for milling should be chosen so as to have optimal leaching. Figure 3.20 shows that milling to time t_5 and milling to time t_6 gives the same leaching time for a desired leach product.

The integrated leaching curves show that there are unique set times for leaching and milling. The leach curves form an envelope with a region above and a region below the envelope. The envelope of the Attainable Region is shown in figure 3.21. Above the leach curves is the achievable region termed the Attainable Region. Any mass fraction distribution of leachable component remaining can be obtained corresponding to a specified period of time within the shaded region can be attained. The envelope of the Attainable Region is formed by joining the outer parts of the individual leach curves. The optimal operation of the process of leaching is along the envelope.

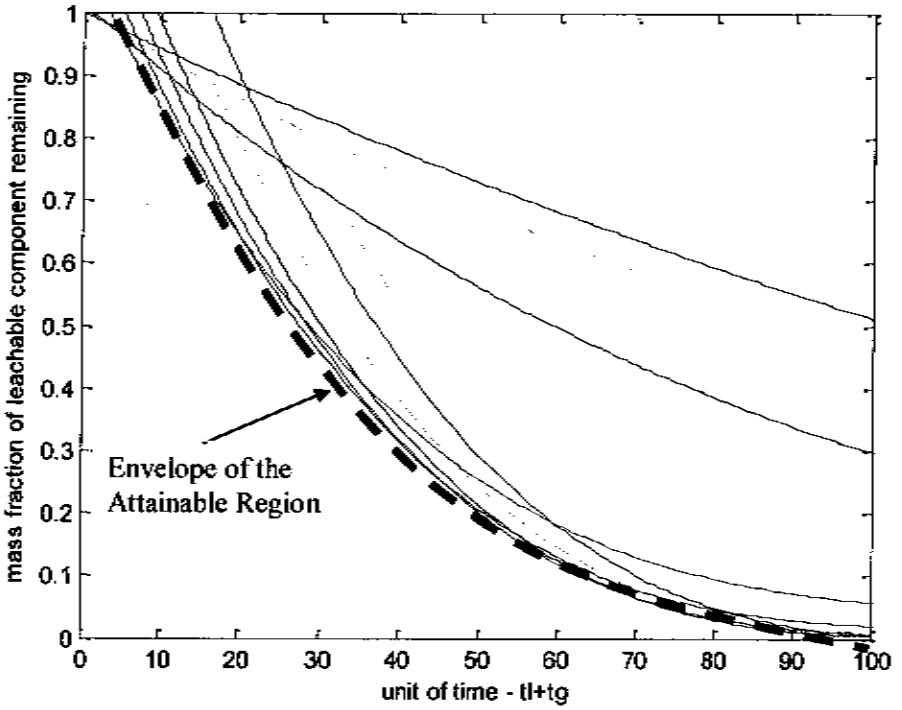

Figure 3.21- Attainable region (shaded region) of the comminution - leaching process

The envelope shows the boundary is the limit for the combined leaching and comminution processes. The leaching and comminution process. The leaching and comminution process occur within the envelope and cannot occur outside the envelope. All the combined leaching and comminution process occurs in the space above the dotted line.

3.4.1 Other Leaching Models

Outlined in this section is the sensitivity of the model developed to changes in leaching kinetics of the sample, i.e. the control regime. The sensitivity of the model is also tested to changes in the reaction time of the particles in the size classes Plots of the other control regimes namely ash layer and diffusion controlling are given in figures 3.22 and 3.23.

3.4.1.1 Ash and Diffusion Control Leaching Regimes

If we follow the same thought experiment as described in section 3.4 i.e. material is charged into a comminution process and allowed to grind for a time t_g and the charged to a leaching process and leached for a time t_l. In this scenario we assume that the particles follow an ash layer controlled leaching reaction, the leach curves yielded are shown in figure 3.22. Using the same color code for curves as given in Table 5.

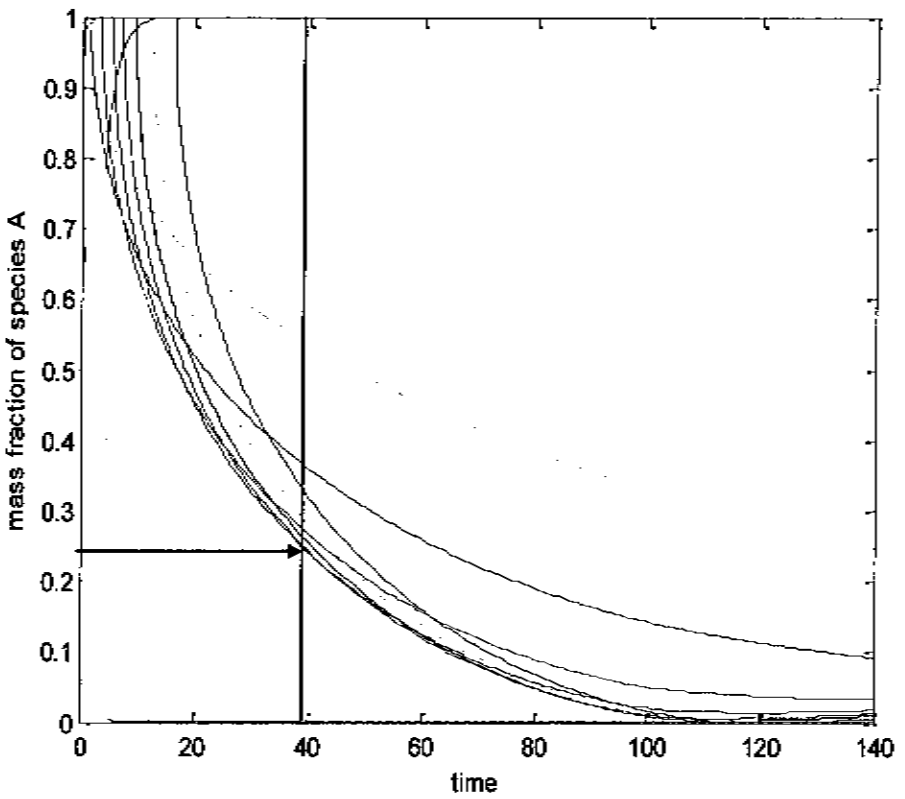

Figure 3.22 – Resultant Leach Curves for ash layer control regime

The leaching curves are steeper, with the ash layer control of dissolution of species A occurring faster than if chemical reaction controls. The time taken for diffusion controlled leaching reactions show that the reaction goes to completion at a rate slower than the other regimes for a 75% dissolution target.

Knowing the control regime also has a significant effect on the milling kinetics. The ash layer control regime occurs faster than the chemical controlled regime and the diffusion controlled regime is the slowest of the three. Therefore milling should be to a greater extent for the diffusion controlled regime and less extent for the ash layer controlled regime.

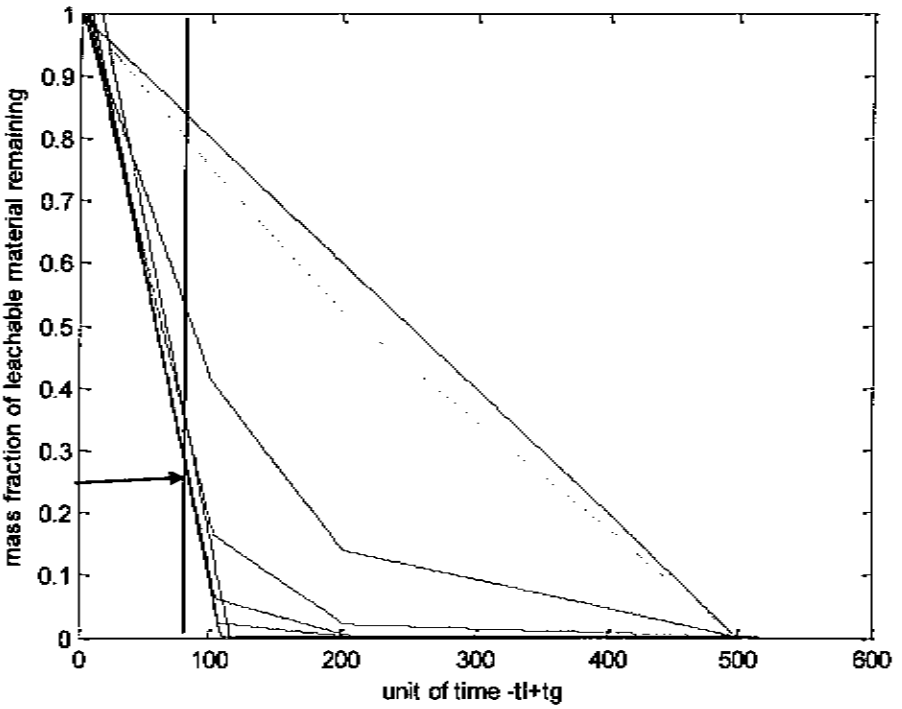

Figure 3.23– Resultant Leach Curves for diffusion control regime

3.4.1.2 Sensitivity to time to completion

Assuming the sizes of the classes 1, 2 and 3 are vastly different thus resulting in reaction time differences of the ratio 50:2:1, yields leach curves shown in figure 3.24 assuming chemical reaction is the control regime.

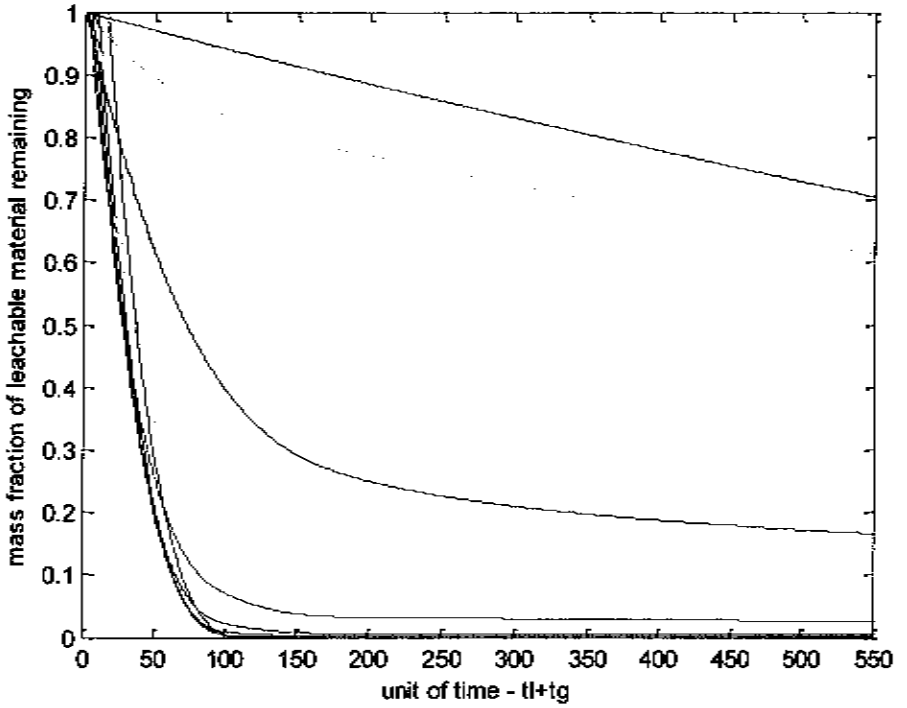

Figure 3.24– Resultant Leach Curves for Chemical Reaction Control regime for residence time ratio 5000:200:100

Figure 3.24 shows a scenario where there is very coarse material that is fed into the leaching reactor. The coarse material has a much larger reaction time as compared to the other particle size classes. If we assume target dissolution of 75%, the graph shows that dissolution for curves t_5, t_6, and t_7 reach the target point at similar times. Hence the presence of very coarse material does not affect the processing time of the particles once the comminution process has reduced the mass fraction of the coarse material to a low value. If the smaller sized particles constitute the majority of the sample, the coarse material does not significantly impact the leaching kinetics.

3.4.2 Selectivity During Leaching

Consider the thought experiment outlined in section 3.2: The material ground for a time (t_g) in the batch mill is then charged into a batch leaching reactor where it undergoes leaching for a further time interval t_l. Each size class is subject to varying leaching rates due mainly to the different radii of the particles. We initially assumed that only the mineral of interest goes into solution, if we lift that constraints and assume that there are two or more metals that are going into solution we can obtain leaching curves that predict the leaching behavior of the minerals.

Consider the following: If we assume that the sample contains two species of metals with the same grinding characteristics that leach at different rates, and leach independently of each other, simulation of the selectivity of metal A compared to B can be done. Figure 3.25 shows how the leach curves of species A versus species B are affected by the change in the size distribution of the feed to the leach reactor. Processes whereby one species of metal is required and yet two or more species go into solution possess a great challenge to the process and it is necessary to optimize the process. For the purposes of this example we will assume that: species B leaches 10 times faster than species A, and assume both species follow the *chemical reaction controls* model. The reaction time for complete conversion the ratio 5:2:1 for the class 1, 2 and 3 respectively for both species A and B. Species B is two thirds of the sample and species A is a third of the sample.

Table 6 – Color Codes for selectivity curves

Sampling Times	Color of curve
t_0	Dashed blue
t_1	black
t_2	Yellow
t_3	Magenta
t_4	Cyan
t_5	Green
t_6	Black
t_7	Blue
t_8	Red

We assume the grinding characteristics are similar to those shown in Figure 3.2 and the times of grinding that we consider are the same as those in Table 3. We obtain Figure 3.25 , a graph showing the mass fraction of leachable species A remaining in solution versus mass fraction of leachable species B remaining in solution after the leaching process. Assuming B is the desirable species, specifying the target mass fraction of leachable material remaining to be a mass fraction of 0.1, we find that we obtain varying proportions of species A as t_g is varies.

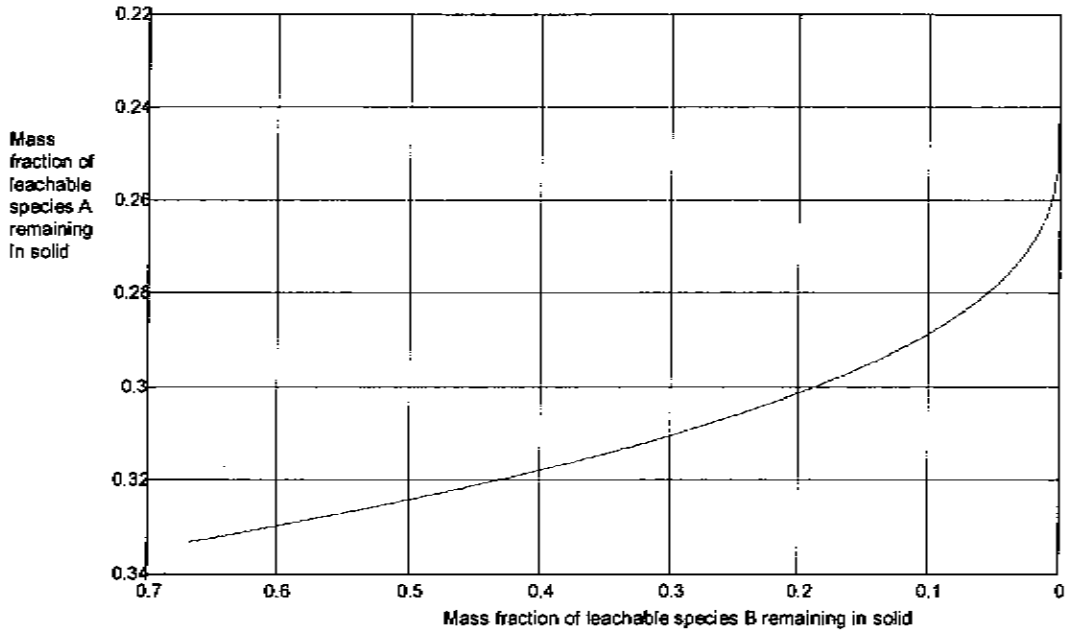

Figure 3.25–Selectivity plot of species A and species B where grinding time at t_0 as defined in table 3

At t_0, no milling has occurred, the sample has particles of size class 1, the graph shows that species B leaches at a very fast rate compared to species A. All the species B is leached out and 0.245 of species A remains in the solid phase. Figure 3.26 show a plot of the mass fraction of leachable species B remaining versus the mass fraction of leachable species A remaining after grinding to t_1 as defined in table 3. Figure 3.25 shows a steeper curve compared to figure 3.26, this shows that grinding the sample has an influence on the dissolution of the species of material in the solution. Figure 3.27 shows the leaching curves of species A versus species B corresponding to grinding times from t_0 to t_{10}.

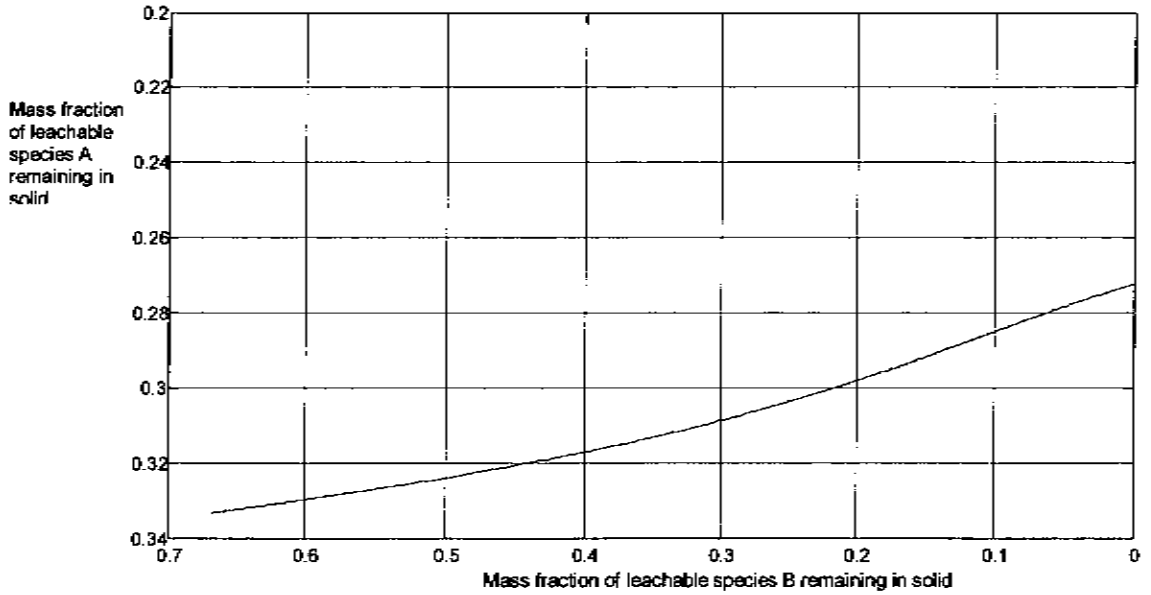

Figure 3.26–Selectivity plot of species A and species B where grinding time at t_1 as defined in table 3

The curves of different colours are defined in table 6.

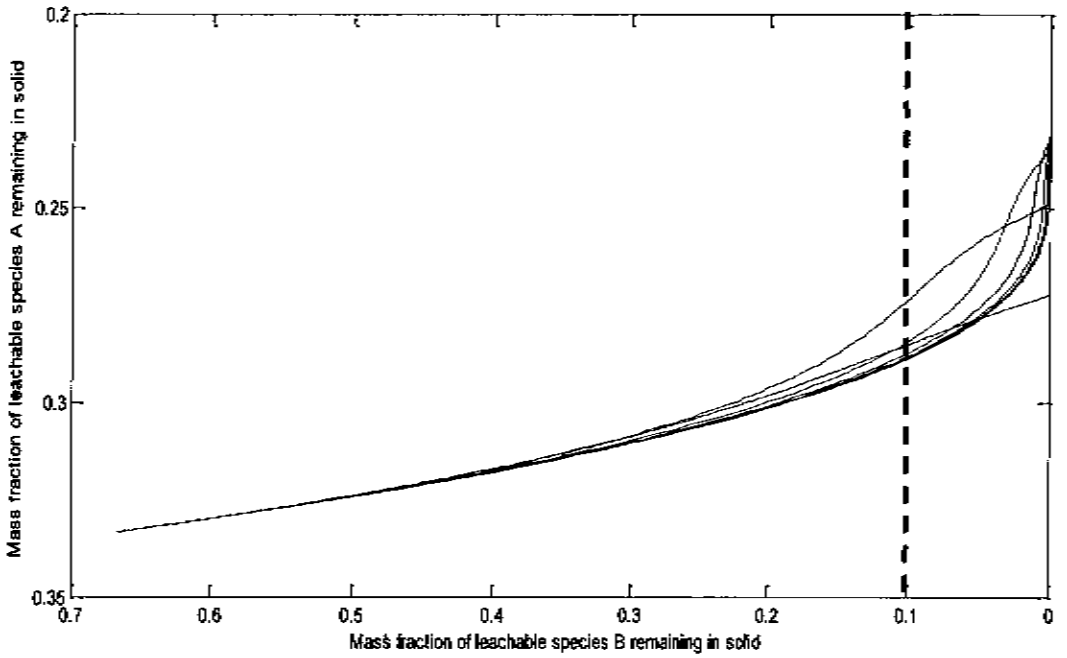

Figure 3.27–Selectivity plot of species A and species B where grinding time is varied from t_1 to t_{10} as defined in table 3

For example: Assuming a target of 0.567, mass fraction of species B is required from the process; this is equal to 0.1 mass fraction of species B is remaining in the solid phase. The t_1 curve shows that quantity of species A remaining in the solid phase will be 0.285.This is slightly higher than the quantity at t_0 showing that grinding the material has an effect on the proportion of A and B leached. At t_2 the mass fraction for species A remaining in solid is 0.275, more of species A goes into solution as compared to the scenario after grinding for a time t_1. At t_3, a mass fraction of 0.273 of species A remains in solid. At t_4, a mass fraction of 0.28 of species A

remains in solid. At t_5, a mass fraction of 0.29 of species A remains in solid. From t_6-t_8 grinding the sample does not significantly affect the proportion of A and B that remains in solid after leaching.

If the main objective for leaching is to make sure that maximum leaching of the desirable species is achieved and the solution contains less of the undesirable species. The graphs show that if a target of 0.567 of species B is required, the least amount of species A is obtained when the sample is milled for a time greater than t_5. Based on the analysis, we deduce that if selectivity of the valuable species is the main objective during leaching, the sample should be ground to point t_5 further than that will not make a difference to the leach results, rather it will result in wastage of energy that would be used for further milling.

3.4.3 Attainable Regions Analysis

Work done by Khumalo et al (2006) has shown that Attainable Regions can be applied to particulate systems like comminution. Leaching is a chemical reaction and the leach tank is a particular type of reactor. In leaching the fundamental processes taking place are reaction and mixing. In deriving the leaching model it was assumed that the leaching system consists of a single particle sizes per class interval and rate of reaction depends on the size of the feed to the leach. These assumptions imply that as soon as the particles enter the leaching reactor they are instantaneously changed hence the rate of leaching depends on the initial size of the particles.

The characteristic vector $c = [x,\tau]$,where x is the mass fraction of the leachable material remaining and τ is the time of leaching and grinding, the kinetics of leaching as shown in figure

3.19 show that as time progresses there is a decrease in the rate of leaching. There is a steep gradient at the beginning of the reaction corresponding to a high reaction rate. As the particles shrink there is a decrease in the rate of reaction corresponding to a flatter curve. According to the Attainable Regions Analysis the concavity of the leaching curve should be removed by mixing. However the leaching plots do not show concavity. This shows that mixing does not contribute to greater efficiency of the leaching process. The slight concavities in the other regimes i.e. ash layer and chemical reaction controls show that mixing is required towards the end of the leaching process.

The Chemical Reaction controlled regime has a straight line at the beginning of the curve showing that it's a plug flow region. And towards the end of the leaching cycle the slight concavity is removed by mixing hence a continuous stirred tank reactor would be used. The same analysis applies for ash layer controlled regime, however there are no concavities in the diffusion controlled regime showing that there is no mixing required and hence the reaction can be completed using a PFR.

3.4.5 LEACHING MODEL BASED ON THE ZINC SULPHIDE LEACHING SYSTEM

The model outlined in section 3.4 was used to predict the leaching kinetics in a real system. The leaching process is modeled based on the leaching kinetics developed by S Aydogan, A Aras and M Canbazoglu and published in the Chemical Engineering Journal(114) in 2005 from page 67-72. Aydogan et al (2005) leached ZnS with ferric chloride solutions. The dissolution of ZnS in acidic $FeCl_3$ solution follows the oxidation-reduction reaction shown in equation 3.2.

$$ZnS + 2Fe^{3+} = Zn^{2+} + 2Fe^{2+} + S^{0} \quad 3.2$$

Aydogan et al developed a model that describes the behavior of the ZnS leaching system. The researchers proposed that the leaching process followed the shrinking core model of leaching where the chemical reaction control was the controlling regime. The process is assumed to be controlled entirely by the events occurring within the particles.

3.4.5.1. Background of Zinc Sulphide Leaching

Zinc is primarily sourced from Sphalerite (ZnS) which is an ore that is mainly associated with metal sulphide minerals such as chalcopyrite ($CuFeS_2$), galena (PbS) and pyrite (FeS_2). In typical mineral processing operations, the ZnS ore is milled then undergoes froth flotation where the ZnS is collected in a concentrate which contain more than 50% Zn. Convectional Zn metal recovery from the ZnS ore involves roasting the sulphide concentrates in air at a temperature of about 925°C to convert the sulphide material to zinc calcine (ZnO). The calcine formed is then leached in dilute sulphuric acid. The leach solution then filtered form the gangue material and then subjected to electro winning processes thus depositing Zn metal. This method of production has found great success in production of Zinc; however the roasting process followed by the electrowinning is not efficient in the utilization of small and complex ZnS deposits. In addition the roasting process results in the production of SO_2 which is a pollutant. Hence to adhere to environmental restrictions alternate methods of producing Zn from ZnS have been researched on, one of them being the direct leaching of ZnS. The elimination of the roasting stage is a very attractive processing route from a technical, economical and environmental point of view.

Aydogan et al (2005) developed a model that describes the behavior of the ZnS leaching system. The researchers proposed that the leaching process followed the shrinking core model of leaching where the chemical reaction controls was the controlling regime. Aydogan et al (2005) found the rate equation of the leaching process to be as follows:

$$[1-(1-\alpha)^{1/3}] = k_0 (Fe^{3+})^{0.36} (\rho_{s/L})^{-0.33} r_0^{-0.97} \exp^{(-45300/RT)} t$$

Ayodogan et al (2005) did a chemical analysis of a ZnS concentrate to find the percentage Zn in the various size class distributions and the results are shown in table 6:

Table 6 – Chemical Analysis of Zinc Sulphide sample

Particle Size (μm)	Zn %
-212+106	57.87
-106+75	59.97
-75+45	61.73
-45+38	57.70
-38	39.53

In order to model a three particle system the medians of the first three particle size distributions are used to fit the ZnS data into the model developed. Hence size class 1 would be -212+106μm the median of the range is 159 μm, size class 2 would be -106+75 μm the median of the range

90.5 μm, size class 3 would be -75+45 μm and the median of the range 60 μm. For the purposes of illustration the first three size classes will be considered.

The leach parameters were defined as follows:

The density of the solid liquid mixture ($\rho_{s/L}$) =1.2g/l

Ferric ion concentration of the lixiviate [Fe^{3+}] =1M

Reaction constant (k_0) = $3.37x10^6 s^{-1}$

Universal gas constant (R) = $8.314 N\mu m^{-2}K^{-1}$l

Temperature (T) = 323K

At t_o, the mass fraction of particles in size class 1 is (m_1) =1. It is assumed only particles in size class one are charged into the reactor, leaching occurs fairly slowly. At any time t, there will be varying proportions of the particles in class 1, 2 or 3 are mixed. The individual leach curves at a time t_n showed varying steepness as a result of the different feed distributions therefore the resultant curves also have varying steepness's. A series of leach curves plotted at varying times and based on varying proportions of size class 1, 2 and 3 are shown. The curves are affected by the relative proportions of the size classes in the feed charged to the leaching reactor as well as the percentage of Zn in the class size range.

At time t_n greater than t_0, the leaching curves become progressively steeper, This is due to the increase in the proportion of the amount of material with particles of size class 3. The particles in size class 3 accelerate the conversion rate. As time progresses the larger particle in the mixture of

solids effect the reduction of the conversion rate resulting in a less steep slope at the end of leaching.

3.4.5.2 Analysis of Integrated Comminution and Leaching for the ZnS System

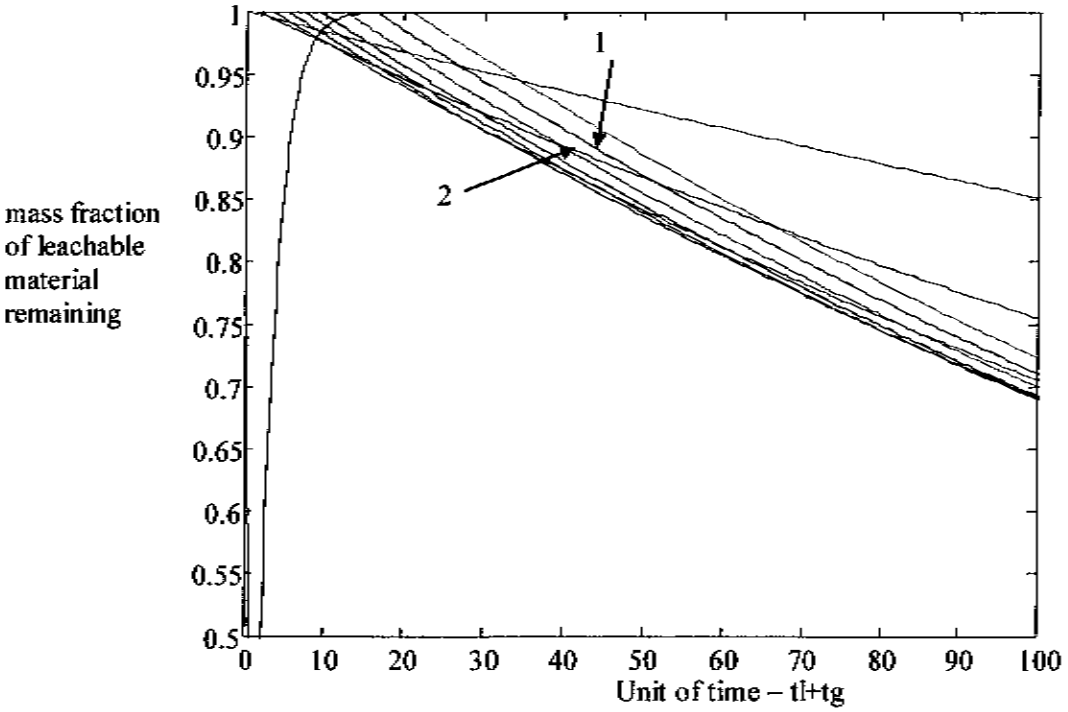

Figure 3.28 Resultant leach curves for ZnS leaching system for time between 0 and 100 time units.

Assuming for the sake of this discussion that a target of about 15% dissolution of ZnS is required, figure 3.4 shows that curves 1 and 2 get to the target point at the same time. Line 1 and

2 are leach curves that result from leaching of comminution products with varying proportions of size class 1,2 and 3. Line 2 represents a scenario where there is present more of the larger particles and Line 1 shows where there are less of the larger particles. Hence the curves show that for a target of 15% dissolution of ZnS there is no need to grind the material to a point where leaching would follow line 1. This is for a low dissolution of ZnS. At higher dissolution there is significant diversion for line 1 and 2. Hence the model can be used to predict the comminution product obtained using the list energy of comminution that can give the required dissolution after leaching.

CHAPTER FOUR – CONCLUSION AND RECOMMENDATIONS

4.1 CONCLUSION

In summary the aim of this thesis was to investigate the integration of the comminution and leaching processes and to investigate the optimization of the integrated processes. It has been shown that the processes can be integrated. The leaching and comminution processes can be considered as a combined unit. The Attainable Region analysis as investigated in this study gives us an envelope showing the boundary of operation of the process. We can deduce that not much mixing is required for the leaching to be effective.

Comminution time should be based on a targeted leach extraction and not be derived independently. Considerable cost savings can be realized by treating the two processes as an integrated combined system. Establishing a target particle size distribution for the comminution process without considering the leaching process may prove to be an inefficient option. Finer grinding may speed up leaching but expend too much energy in comminution. Finer particles can also prove to be problematic in the comminution and down-stream processing circuits. The model predicts that there is an optimal size distribution for effective leaching to take place. The model shows that different size classes can be mixed to obtain a target leach output. Combining the two process steps opens possibilities to run the process more effectively and efficiently.

4.2 RECOMMMENDATIONS

Mechanochemical processing systems are of central importance in the mineral processing sector. It is therefore of critical importance that models be developed that choose to integrate both the leaching and the comminution processes. Such models would be beneficial in prediction the behavior of the processing systems in reaction mills and can form the basis of design of a reaction mill and classical milling and circuits.

The understanding of a comminution process and its effects on the proceeding processes like flotation, leaching, smelting etc is in its infancy and there are a lot of opportunities to extend this work. More unit operations can be added to the cascade of processes and integrated so as to find the optimum operating conditions for the entire process.

The analysis considered only first order leaching and comminution process. More work can be done by analyzing higher order systems.

REFERENCES

1. Austin L G., Klimpel R R., Luckie P T., (1984). Process Engineering for Size Reduction: Ball Milling, Guinn Printing Inc., Hoboken , New Jersey, United States of America.
2. Aydogan S., Aras A,. Canbazoglu M., (2005). Dissolution Kinetics of Sphalerite in Acidic Ferric Chloride Leaching. Chemical Engineering Journal 114 (67 -72)
3. Bade S. And Hoffman U (1996). Modelling of the simultaneous comminution and chemical reaction in a non catalytic gas-solid batch reactor. Chemical Engineering Science, 52 (16).
4. Bade S, Hoffman U (1997). Developing a new reactor for combined comminution and chemical reaction. Chemical Engineering Communication
5. Bilgili E, Yepes J, Scarlett B (2005). Formulation of a non liner framework for population balance modelling of batch grinding: Beyond first order kinetics. Chemical Engineering Science (61).
6. Caballero J A, Odjo A and Grossman EG.(2007) Flowsheet Optimisation with Implicit Models and Complex Cost and Size Functions using Chemical Process Simulators. AIChe Journal 53(9)
7. Crundwell F K., (1995). Progress in Mathematical Modeling of Leaching Reactors. Hydrometallurgy 321-335.
8. Dixon D G., Hendrix J L., (1993). A General Model for Leaching of One or More Solid Reactants from Porous Ore Particles. Metallurgical Transactions B (157-168)

9. Glasser D., Hildebrandt D., and Crowne, C. (1990). The geometry of the attainable region generated by reaction and mixing with and without constraints. Industrial and Engineering Chemistry Research, 29(1).

10. Hildebrandt D., and Glasser, D. (1990). The attainable Region and optimal reactor structures. Chemical Engineering Science, 45(8).

11. Horn F. (1964). Attainable and non attainable regions in chemical reaction technique. Third European Symposium on Chemical Reaction Engineering. Pergamon Press Ltd., Great Britain.

12. Khumalo N, (2007), The Application of Attainable Regions Analysis in Comminution, Republic of South Africa: University Of Witwatersrand.

13. Levenspiel, Octave, 1972. Chemical Reaction Engineering, Second ed. John Wiley and Sons, Inc., New York.

14. Melody TP and Williams MC (1992). Problems in population balance modeling of wet grinding. Powder Technology, 71(3)

15. N Khumalo., D Glasser., D Hildebrandt., B Hansberger., S Kauchali., 2006. The application of attainable Region analysis to comminution. Chemical Engineering Science 61.

16. Philip K., Gbor., Charles Q., Jia,. (2004). Critical Evaluation of Coupling Particle Size Distribution with the Shrinking Core Model. Chemical Engineering Science 59

17. Sowerby (2002). On-Line Measurement and Control in Sustainable Mineral Processing and Energy Production. Australian Academy for Technological Sciences and Engineering, 120.

18. Wen, C.Y., 1968. Noncatalytic heterogeneous solid fluid reaction models. Industrial and Engineering Chemistry 60 (8), pp. 34–54.

19. Williams MC., Melody TP, (1997). Population Balance Models and Self Similar Size Distributions. Minerals Engineering, 10(2)

20. Yagi, S., Kunii, D., 1955. Studies on combustion of carbon particles in flames and fluidized beds. In: Fifth Symposium (International) on Combustion, Reinhold, New York, pp. 231–244.

APPENDICES

COMMINUTION MODEL

```
function dm=PBal(t,m)
global c
global s
dm=zeros(2,1);

k1=1;
k2=0.5;

b=0.9;


dm(1)= -k1*m(1);
dm(2)= -k2*m(2)+k1*b*m(1);
% dm(3)=1-dm(1)-dm(2);



clc;clear all

init=[1 0];
tspan=[0.00001 600];


[t,m]=ode45('PBal',tspan,init);
hold on
xlabel('time')
ylabel('mass fraction')

figure(2)
hold on

plot(t,m(:,1),'k')

hold on
plot(t,m(:,2),'k')

for i = 1:length(m(:,1))
    m3(i) = 1-(m(i,1)+m(i,2));
end

hold on
plot (t,m3,'k')

m = [m m3'];
xlabel('time')
ylabel('mass fraction')

figure (3)
plot(m(:,1),m(:,2),'--')
```

LEACHING MODEL

```
for i = 1:length(c)
     tleach1(i)=t(20)+t(i);
%  c1(i) = 1-(sin(1/3*asin(1-2*t(i)/500))+1/2)^3;
    c1(i) = (1-(exp(-t(i)/500)));
% c1(i) = t(i)/500;

  mleach1(i) = m(20,1)*(1-c1(i));

if mleach1(i) < 0
```

```
    mleach1(i) =0;
    end
end
figure(1)
hold on
plot (tleach1,mleach1,'b')

for i = 1:length(c)
     tleach1(i)=t(20)+t(i);
%  c2(i) = 1-(sin(1/3*asin(1-2*t(i)/200))+1/2)^3;
    c2(i) = (1-(exp(-t(i)/200)));
% c2(i) = t(i)/200;

  mleach2(i) = m(20,2)*(1-c2(i));
  if mleach2(i) < 0
    mleach2(i) =0;
    end
end

figure(1)
hold on
plot (tleach1,mleach2,'r')

for i = 1:length(c)

        tleach1(i)=t(20)+t(i);
%    c3(i) = 1-(sin(1/3*asin(1-2*t(i)/100))+1/2)^3;
% c3(i) = t(i)/100;
 c3(i) = (1-(exp(-t(i)/100)));
  mleach3(i) = m(20,3)*(1-c3(i));
if mleach3(i) < 0
    mleach3(i) =0;
    end
end

figure(1)
hold on
plot (tleach1,mleach3,'k')

for i = 1:length(c)
    mleach4(i)= m(20,3)*(1-c3(i))+ m(20,2)*(1-c2(i))+  m(20,1)*(1-c1(i));
    if mleach4(i) < 0
    mleach4(i) =0;
    end


    end

figure(2)
hold on
plot (tleach1,mleach4,'--')

figure (3)
plot(mleach2,mleach1,'--')


for i = 1:length(c)



% c1(i) = 1-(sin(1/3*asin(1-2*t(i)/500))+1/2)^3;
  c1(i) = (1-(exp(-t(i)/500)));
% c1(i) = t(i)/500;
  tleach2(i)=t(26)+t(i);
if c1(i)== 0.00002
    pause
end
  mleach5(i) = m(26,1)*(1-c1(i));
if mleach5(i) < 0
    mleach5(i) =0;
    end
```

```
end

figure(1)
hold on
plot (tleach2,mleach5,'r')

for i = 1:length(c)

%  c2(i) = 1-(sin(1/3*asin(1-2*t(i)/200))+1/2)^3;
c2(i) = (1-(exp(-t(i)/200)));
% c2(i) = t(i)/200;
  tleach2(i)=t(26)+t(i);
  mleach6(i) = m(26,2)*(1-c2(i));
  if mleach6(i) < 0
    mleach6(i) = 0;
    end
end

figure(1)
hold on
plot (tleach2,mleach6,'b')

for i = 1:length(c)


%   c3(i) = 1-(sin(1/3*asin(1-2*t(i)/100))+1/2)^3;
c3(i) = (1-(exp(-t(i)/100)));
% c3(i) = t(i)/100;
  tleach2(i)=t(26)+t(i);
  mleach7(i) = m(26,3)*(1-c3(i));
  if mleach7 (i) < 0
    mleach7(i) =0;
    end
end

figure(1)
hold on
plot (tleach2,mleach7,'k')

for i = 1:length(c)
    mleach8(i)= m(26,3)*(1-c3(i))+ m(26,2)*(1-c2(i))+  m(26,1)*(1-c1(i));
if mleach8(i) < 0
    mleach8(i) =0;
    end
end
figure(2)
hold on
plot (tleach2,mleach8,'y')

figure (3)
plot(mleach6,mleach5,'y')


for i = 1:length(c)

%  c1(i) = 1-(sin(1/3*asin(1-2*t(i)/500))+1/2)^3;
 c1(i) = (1-(exp(-t(i)/500)));
% c1(i) = t(i)/500;
  tleach3(i)=t(30)+t(i);
  mleach9(i) = m(30,1)*(1-c1(i));
  if mleach9(i) < 0
    mleach9(i) =0;
    end
end


figure(1)
hold on
plot (tleach3,mleach9,'r')

for i = 1:length(c)
```

```
%  c2(i) = 1-(sin(1/3*asin(1-2*t(i)/200))+1/2)^3;
c2(i) = (1-(exp(-t(i)/200)));
% c2(i) = t(i)/200;
  tleach3(i)=t(30)+t(i);
    mleach10(i) = m(30,2)*(1-c2(i));
    if mleach10(i) < 0
    mleach10(i) =0;
    end
end

figure(1)
hold on
plot (tleach3,mleach10,'b')

for i = 1:length(c)
%     c3(i) = 1-(sin(1/3*asin(1-2*t(i)/100))+1/2)^3;
  c3(i) = (1-(exp(-t(i)/100)));
% c3(i) = t(i)/100;
  tleach3(i)=t(30)+t(i);
  mleach11(i) = m(30,3)*(1-c3(i));
if mleach11(i) < 0
    mleach11(i) =0;
    end

end

figure(1)
hold on
plot (tleach3,mleach11,'k')

for i = 1:length(c)
    mleach12(i)= m(30,3)*(1-c3(i))+ m(30,2)*(1-c2(i))+  m(30,1)*(1-c1(i));
if mleach12(i) < 0
    mleach12(i) =0;
   end
end
figure(2)
hold on
plot (tleach3,mleach12,'m')

figure (3)
plot(mleach9,mleach10,'m')


for i = 1:length(c)

% c1(i) = 1-(sin(1/3*asin(1-2*t(i)/500))+1/2)^3;
 c1(i) = (1-(exp(-t(i)/500)));
% c1(i) = t(i)/500;
  tleach4(i)=t(40)+t(i);
  mleach13(i) = m(40,1)*(1-c1(i));
if mleach13(i) < 0
    mleach13(i) =0;
    end
end

figure(1)
hold on
plot (tleach4,mleach13,'r')

for i = 1:length(c)
%   c2(i) = 1-(sin(1/3*asin(1-2*t(i)/200))+1/2)^3;
c2(i) = (1-(exp(-t(i)/200)));
% c2(i) = t(i)/200;
  tleach4(i)=t(40)+t(i);
  mleach14(i) = m(40,2)*(1-c2(i));
if mleach14(i) < 0
    mleach14(i) =0;
    end
```

```
end

figure(1)
hold on
plot (tleach4,mleach14,'b')

for i = 1:length(c)
%    c3(i) = 1-(sin(1/3*asin(1-2*t(i)/100))+1/2)^3;
c3(i) = (1-(exp(-t(i)/500)));
% c3(i) = t(i)/100;
  tleach4(i)=t(40)+t(i);
  mleach15(i) = m(40,3)*(1-c3(i));
if mleach15(i) < 0
    mleach15(i) =0;
    end
end

figure(1)
hold on
plot (tleach4,mleach15,'k')

for i = 1:length(c)
    mleach16(i)= m(40,3)*(1-c3(i))+ m(40,2)*(1-c2(i))+  m(40,1)*(1-c1(i));
if mleach16(i) < 0
    mleach16(i) =0;
    end
end
figure(2)
hold on
plot (tleach4,mleach16,'c')
figure (3)
plot(mleach13,mleach14,'c')



for i = 1:length(c)
%   c1(i) = 1-(sin(1/3*asin(1-2*t(i)/500))+1/2)^3;
 c1(i) = (1-(exp(-t(i)/500)));
% c1(i) = t(i)/500;
  tleach5(i)=t(50)+t(i);
  mleach17(i) = m(50,1)*(1-c1(i));
if mleach17(i) < 0
    mleach17(i) =0;
   end
end

figure(1)
hold on
plot (tleach5,mleach17,'r')

for i = 1:length(c)
%   c2(i) = 1-(sin(1/3*asin(1-2*t(i)/200))+1/2)^3;
c2(i) = (1-(exp(-t(i)/200)));
% c2(i) = t(i)/200;
  tleach5(i)=t(50)+t(i);
  mleach18(i) = m(50,2)*(1-c2(i));
  if mleach18(i) < 0
    mleach18(i) =0;
    end
end

figure(1)
hold on
plot (tleach5,mleach18,'b')

for i = 1:length(c)
%    c3(i) = 1-(sin(1/3*asin(1-2*t(i)/100))+1/2)^3;
c3(i) = (1-(exp(-t(i)/100)));
% c3(i) = t(i)/100;
  tleach5(i)=t(50)+t(i);
  mleach19(i) = m(50,3)*(1-c3(i));
```

```
  if mleach19(i) < 0
    mleach19(i) =0;
    end
end

figure(1)
hold on
plot (tleach5,mleach19,'k')

for i = 1:length(c)
    mleach20(i)= m(50,3)*(1-c3(i))+ m(50,2)*(1-c2(i))+  m(50,1)*(1-c1(i));
if mleach20(i) < 0
    mleach20(i) =0;
    end
end
figure(2)
hold on
plot (tleach5,mleach20,'b')
figure (3)
plot(mleach17,mleach18,'b')


for i = 1:length(c)

%  c1(i) = 1-(sin(1/3*asin(1-2*t(i)/500))+1/2)^3;
 c1(i) = (1-(exp(-t(i)/500)));
% c1(i) = t(i)/500;

  tleach6(i)=t(60)+t(i);
    mleach21(i) = m(60,1)*(1-c1(i));
    if mleach21(i) < 0
    mleach21(i) =0;
    end
end

figure(1)
hold on
plot (tleach6,mleach21,'r')

for i = 1:length(c)
%   c2(i) = 1-(sin(1/3*asin(1-2*t(i)/200))+1/2)^3;
c2(i) = (1-(exp(-t(i)/200)));
% c2(i) = t(i)/200;
  tleach6(i)=t(60)+t(i);
  mleach22(i) = m(60,2)*(1-c2(i));
if mleach22(i) < 0
    mleach22(i) =0;
    end
end

figure(1)
hold on
plot (tleach6,mleach22,'b')

for i = 1:length(c)
%     c3(i) = 1-(sin(1/3*asin(1-2*t(i)/100))+1/2)^3;
 c3(i) = (1-(exp(-t(i)/100)));
% c3(i) = t(i)/100;
  tleach6(i)=t(60)+t(i);
  mleach23(i) = m(60,3)*(1-c3(i));
  if mleach23(i) < 0
    mleach23(i) =0;
    end
end

figure(1)
hold on
plot (tleach6,mleach23,'k')

for i = 1:length(c)
    mleach24(i)= m(60,3)*(1-c3(i))+ m(60,2)*(1-c2(i))+  m(60,1)*(1-c1(i));
```

```
if mleach24(i) < 0
    mleach24(i) =0;
    end
end
figure(2)
hold on
plot (tleach6,mleach24,'g')

figure (3)
plot(mleach21,mleach22,'g')


for i = 1:length(c)
%  c1(i) = 1-(sin(1/3*asin(1-2*t(i)/500))+1/2)^3;
 c1(i) = (1-(exp(-t(i)/500)));
% c1(i) = t(i)/500;
  tleach7(i)=t(70)+t(i);
    mleach25(i) = m(70,1)*(1-c1(i));
if mleach25(i) < 0
    mleach25(i) =0;
    end
end

figure(1)
hold on
plot (tleach7,mleach25,'r')

for i = 1:length(c)
%   c2(i) = 1-(sin(1/3*asin(1-2*t(i)/200))+1/2)^3;
%   c2(i) = 3*(t(i)/150)-6*(t(i)/150)^2+6*(t(i)/150)^3*(1-exp(-150/t(i)));
 c2(i) = (1-(exp(-t(i)/200)));
% c2(i) = t(i)/200;
  tleach7(i)=t(70)+t(i);
  mleach26(i) = m(70,2)*(1-c2(i));
if mleach26(i) < 0
    mleach26(i) =0;
    end
end

figure(1)
hold on
plot (tleach7,mleach26,'b')

for i = 1:length(c)
%     c3(i) = 1-(sin(1/3*asin(1-2*t(i)/100))+1/2)^3;
c3(i) = (1-(exp(-t(i)/100)));
% c3(i) = t(i)/100;
  tleach7(i)=t(70)+t(i);
  mleach27(i) = m(70,3)*(1-c3(i));
  if mleach27(i) < 0
    mleach27(i) =0;
    end
end

figure(1)
hold on
plot (tleach7,mleach27,'k')

for i = 1:length(c)
    mleach28(i)= m(70,3)*(1-c3(i))+ m(70,2)*(1-c2(i))+  m(70,1)*(1-c1(i));
if mleach28(i) < 0
    mleach28(i) =0;
    end
end
figure(2)
hold on
plot (tleach7,mleach28,'r')

figure (3)
plot(mleach25,mleach26,'r')
```

```
for i = 1:length(c)

%  c1(i) = 1-(sin(1/3*asin(1-2*t(i)/500))+1/2)^3;
  c1(i) = (1-(exp(-t(i)/500)));
% c1(i) = t(i)/500;
  tleach8(i)=t(80)+t(i);
  mleach29(i) = m(80,1)*(1-c1(i));
  if mleach29(i) < 0
    mleach29(i) = 0;

    end
end

figure(1)
hold on
plot (tleach8,mleach29,'r')

for i = 1:length(c)

%  c2(i) = 1-(sin(1/3*asin(1-2*t(i)/200))+1/2)^3;
c2(i) = (1-(exp(-t(i)/200)));
% c2(i) = t(i)/200;
  tleach8(i)=t(80)+t(i);
  mleach30(i) = m(80,2)*(1-c2(i));
  if mleach30(i) < 0
    mleach30(i) =0;
    end
end

figure(1)
hold on
plot (tleach8,mleach30,'b')

for i = 1:length(c)
%     c3(i) = 1-(sin(1/3*asin(1-2*t(i)/100))+1/2)^3;
c3(i) = (1-(exp(-t(i)/100)));
% c3(i) = t(i)/100;
  tleach8(i)=t(80)+t(i);
  mleach31(i) = m(80,3)*(1-c3(i));
  if mleach31(i) < 0
    mleach31(i) =0;
    end
end

figure(1)
hold on
plot (tleach8,mleach31,'k')

for i = 1:length(c)

mleach32(i)= m(80,3)*(1-c3(i))+ m(80,2)*(1-c2(i))+  m(80,1)*(1-c1(i));
if mleach32(i) < 0
    mleach32(i) =0;
    end
end
figure(2)
hold on
plot (tleach8,mleach32,'-.')

figure (3)
plot(mleach29,mleach30,'-.')


for i = 1:length(c)
%  c1(i) = 1-(sin(1/3*asin(1-2*t(i)/500))+1/2)^3;
 c1(i) = (1-(exp(-t(i)/500)));
% c1(i) = t(i)/500;
  tleach9(i)=t(90)+t(i);
  mleach33(i) = m(90,1)*(1-c1(i));
  if mleach33(i) < 0
    mleach33(i) =0;
```

```
    end
end

figure(1)
hold on
plot (tleach9,mleach33,'r')

for i = 1:length(c)

%  c2(i) = 1-(sin(1/3*asin(1-2*t(i)/200))+1/2)^3;
c2(i) = (1-(exp(-t(i)/200)));
% c2(i) = t(i)/200;
  tleach9(i)=t(90)+t(i);
  mleach34(i) = m(90,2)*(1-c2(i));
if mleach34(i) < 0
    mleach34(i) =0;
    end
end

figure(1)
hold on
plot (tleach9,mleach34,'b')

for i = 1:length(c)
%    c3(i) = 1-(sin(1/3*asin(1-2*t(i)/100))+1/2)^3;
c3(i) = (1-(exp(-t(i)/100)));
% c3(i) = t(i)/100;
  tleach9(i)=t(90)+t(i);
  mleach35(i) = m(90,3)*(1-c3(i));
  if mleach35(i) < 0
    mleach35(i) =0;
    end
end

figure(1)
hold on
plot (tleach9,mleach35,'k')

for i = 1:length(c)

mleach36(i)= m(90,3)*(1-c3(i))+ m(90,2)*(1-c2(i))+  m(90,1)*(1-c1(i));
if mleach36(i) < 0
    mleach36(i) =0;
    end
end
figure(2)
hold on
plot (tleach9,mleach36,'k')

figure (3)
plot(mleach33,mleach34,'k')

for i = 1:length(c)
%   c1(i) = 1-(sin(1/3*asin(1-2*t(i)/500))+1/2)^3;
 c1(i) = (1-(exp(-t(i)/500)));
% c1(i) = t(i)/500;
  tleach10(i)=t(100)+t(i);
  mleach37(i) = m(100,1)*(1-c1(i));
  if mleach37(i) < 0
    mleach37(i) =0;
    end
end

figure(1)
hold on
plot (tleach10,mleach37,'r')

for i = 1:length(c)
%     c2(i) = 1-(sin(1/3*asin(1-2*t(i)/200))+1/2)^3;
c2(i) = (1-(exp(-t(i)/200)));
% c2(i) = t(i)/200;
```

```
  tleach10(i)=t(100)+t(i);
  mleach38(i) = m(100,2)*(1-c2(i));
if mleach38(i) < 0
    mleach38(i) =0;
    end

end

figure(1)
hold on
plot (tleach10,mleach38,'b')

for i = 1:length(c)

%    c3(i) = 1-(sin(1/3*asin(1-2*t(i)/100))+1/2)^3;
c3(i) = (1-(exp(-t(i)/100)));
% c3(i) = t(i)/100;

  tleach10(i)=t(100)+t(i);
  mleach39(i) = m(100,3)*(1-c3(i));
  if mleach39(i) < 0
    mleach39(i) =0;
    end
end

figure(1)
hold on
plot (tleach10,mleach39,'k')

for i = 1:length(c)
 if c(i) < 0
        c(i) = 0;
    end
mleach40(i)= m(100,3)*(1-c3(i))+ m(100,2)*(1-c2(i))+  m(100,1)*(1-c1(i));

if mleach40(i) < 0
    mleach40(i) =0;
   end
end
figure(2)
hold on
plot (tleach10,mleach40,':')


figure (3)
plot(mleach37,mleach38,':')
```

SELECTIVITY MODEL

```
for i = 1:length(c);

tleach9(i)=t(1)+t(i);
%   c1(i) = t(i)/10000;
 c1(i) = 1-((1-t(i)/5000)^(3));
%  c1(i) = 1-(sin(1/3*asin(1-2*t(i)/1000))+1/2)^3;
mleach251(i) =( 1/3*(m(1,1))*(1-c1(i)));
if mleach251(i) < 0
    mleach251(i) =0;
    end

end
    figure(1)
hold on
plot (tleach9,mleach251,'r')
d = 0:0.01:7.5;   % fraction unconverted species 2
for i = 1:length(d)

   tleach9(i)=t(1)+t(i);
```

```
%    c1(i) = t(i)/10000;
 d1(i) = 1-((1-t(i)/500)^(3));
%  d1(i) = 1-(sin(1/3*asin(1-2*t(i)/200))+1/2)^3;
mleach252(i) = 2/3*(m(1,1))*(1-d1(i));
if mleach252(i) < 0
    mleach252(i) =0;
    end
end
    figure(1)
hold on
plot (tleach9,mleach252,'k')


for i = 1:length(c)

tleach9(i)=t(1)+t(i);
%    c1(i) = t(i)/10000;
 c2(i) = 1-((1-t(i)/2000)^3);
%  c2(i) = 1-(sin(1/3*asin(1-2*t(i)/500))+1/2)^3;
mleach261(i) = 1/3*(m(1,2))*(1-c2(i));
if mleach261(i) < 0
    mleach261(i) =0;
    end
end

    figure(1)
hold on
plot (tleach9,mleach261,'y')

for i = 1:length(d)

   tleach9(i)=t(1)+t(i);
%    c1(i) = t(i)/10000;
 d2(i) = 1-((1-t(i)/200)^(3));
%  d2(i) = 1-(sin(2/3*asin(1-2*t(i)/100))+1/2)^3;
mleach262(i) = 2/3*(m(1,2))*(1-d2(i));
if mleach262(i) < 0
    mleach262(i) =0;
    end
end
    figure(1)
hold on
plot (tleach9,mleach262,'m')


for i = 1:length(c)

tleach9(i)=t(1)+t(i);
%    c1(i) = t(i)/10000;
 c3(i) = 1-((1-t(i)/1000)^(3));
% c3(i) = 1-(sin(1/3*asin(1-2*t(i)/250))+1/2)^3;
mleach271(i) = 1/3*(m(1,3))*(1-c3(i));
if mleach271(i) < 0
    mleach271(i) =0;
    end
end

    figure(1)
hold on

plot (tleach9,mleach271,'c')

for i = 1:length(d)

   tleach9(i)=t(1)+t(i);
%    c1(i) = t(i)/10000;
 d3(i) = 1-((1-t(i)/100)^(3));
% d3(i) = 1-(sin(1/3*asin(1-2*t(i)/50))+1/2)^3;
mleach272(i) = 2/3*(m(1,3))*(1-d3(i));
if mleach272(i) < 0
    mleach272(i) =0;
```

```
    end
end
    figure(1)
hold on
plot (tleach9,mleach272,'b')


for i = 1:length(c)

mleach2771(i)= 1/3*(m(1,1))*(1-c1(i))+1/3*(m(1,2))*(1-c2(i))+ 1/3*(m(1,3))*(1-c3(i));

end
figure(2)
hold on
plot (tleach9,mleach2771,'y')

if mleach2771(i) < 0
    mleach2771(i) =0;
    end
for i = 1:length(d)

mleach2772(i)= 2/3*(m(1,1))*(1-d1(i))+2/3*(m(1,2))*(1-d2(i))+ 2/3*(m(1,3))*(1-d3(i));
if mleach2772(i) < 0
    mleach2772(i) =0;
    end
end
figure(2)
hold on
plot (tleach9,mleach2772,'y')


figure(4)
hold on
plot (mleach2772,mleach2771,':')

for i = 1:length(c);

tleach1(i)=t(20)+t(i);
%    c1(i) = t(i)/10000;
 c1(i) = 1-((1-t(i)/5000)^(3));
%  c1(i) = 1-(sin(1/3*asin(1-2*t(i)/1000))+1/2)^3;
mleach11(i) =( 1/3*(m(20,1))*(1-c1(i)));
if mleach11(i) < 0
    mleach11(i) =0;
    end

end
    figure(1)
hold on
plot (tleach1,mleach11,'r')

for i = 1:length(d)

   tleach1(i)=t(20)+t(i);
%    c1(i) = t(i)/10000;
 d1(i) = 1-((1-t(i)/500)^(3));
%  d1(i) = 1-(sin(1/3*asin(1-2*t(i)/200))+1/2)^3;
mleach12(i) = 2/3*(m(20,1))*(1-d1(i));
if mleach12(i) < 0
    mleach12(i) =0;
    end
end
    figure(1)
hold on
plot (tleach1,mleach12,'k')


for i = 1:length(c)
```

```
tleach1(i)=t(20)+t(i);
%    c1(i) = t(i)/10000;
 c2(i) = 1-((1-t(i)/2000)^3);
%  c2(i) = 1-(sin(1/3*asin(1-2*t(i)/500))+1/2)^3;
mleach21(i) = 1/3*(m(20,2))*(1-c2(i));
if mleach21(i) < 0
    mleach21(i) =0;
    end
end

    figure(1)
hold on
plot (tleach1,mleach21,'y')

for i = 1:length(d)

   tleach1(i)=t(20)+t(i);
%    c1(i) = t(i)/10000;
 d2(i) = 1-((1-t(i)/200)^(3));
%  d2(i) = 1-(sin(2/3*asin(1-2*t(i)/100))+1/2)^3;
mleach22(i) = 2/3*(m(20,2))*(1-d2(i));
if mleach22(i) < 0
    mleach22(i) =0;
    end
end
    figure(1)
hold on
plot (tleach1,mleach22,'m')


for i = 1:length(c)

tleach1(i)=t(20)+t(i);
%    c1(i) = t(i)/10000;
 c3(i) = 1-((1-t(i)/1000)^(3));
% c3(i) = 1-(sin(1/3*asin(1-2*t(i)/250))+1/2)^3;
mleach31(i) = 1/3*(m(20,3))*(1-c3(i));
if mleach31(i) < 0
    mleach31(i) =0;
    end
end

    figure(1)
hold on

plot (tleach1,mleach31,'c')

for i = 1:length(d)

   tleach1(i)=t(20)+t(i);
%    c1(i) = t(i)/10000;
 d3(i) = 1-((1-t(i)/100)^(3));
% d3(i) = 1-(sin(1/3*asin(1-2*t(i)/50))+1/2)^3;
mleach32(i) = 2/3*(m(20,3))*(1-d3(i));
if mleach32(i) < 0
    mleach32(i) =0;
    end
end
    figure(1)
hold on
plot (tleach1,mleach32,'b')



for i = 1:length(c)

mleach331(i)= 1/3*(m(20,1))*(1-c1(i))+1/3*(m(20,2))*(1-c2(i))+ 1/3*(m(20,3))*(1-c3(i));
if mleach331(i) < 0
    mleach331(i) =0;
    end
end
```

```
figure(2)
hold on
plot (tleach1,mleach331,'y')


for i = 1:length(d)

mleach332(i)= 2/3*(m(20,1))*(1-d1(i))+2/3*(m(20,2))*(1-d2(i))+ 2/3*(m(20,3))*(1-d3(i));
if mleach332(i) < 0
    mleach332(i) =0;
    end
end
figure(2)
hold on
plot (tleach1,mleach332,'y')


figure(4)
hold on
plot (mleach332,mleach331,'k')


for i = 1:length(c)

tleach2(i)=t(26)+t(i);
%   c1(i) = t(i)/10000;
 c1(i) = 1-((1-t(i)/5000)^(3));
%  c1(i) = 1-(sin(1/3*asin(1-2*t(i)/1000))+1/2)^3;
mleach41(i) = 1/3*(m(26,1))*(1-c1(i));
if mleach41(i) < 0
    mleach41(i) =0;
    end
end

    figure(1)
hold on
plot (tleach2,mleach41,'r')

for i = 1:length(d)

   tleach2(i)=t(26)+t(i);
%   c1(i) = t(i)/10000;
 d1(i) = 1-((1-t(i)/500)^(3));
%  d1(i) = 1-(sin(1/3*asin(1-2*t(i)/200))+1/2)^3;
mleach42(i) = 2/3*(m(26,1))*(1-d1(i));
if mleach42(i) < 0
    mleach42(i) =0;
    end
end
    figure(1)
hold on
plot (tleach2,mleach42,'k')



for i = 1:length(c)

tleach2(i)=t(26)+t(i);
%   c1(i) = t(i)/10000;
 c2(i) = 1-((1-t(i)/2000)^(3));
%  c2(i) = 1-(sin(1/3*asin(1-2*t(i)/500))+1/2)^3;
mleach51(i) = 1/3*(m(26,2))*(1-c2(i));
if mleach51(i) < 0
    mleach51(i) =0;
    end
end

    figure(1)
hold on
plot (tleach2,mleach51,'y')
```

```
for i = 1:length(d)

   tleach2(i)=t(26)+t(i);
%   c1(i) = t(i)/10000;
 d2(i) = 1-((1-t(i)/200)^(3));
% d2(i) = 1-(sin(1/3*asin(1-2*t(i)/100))+1/2)^3;
mleach52(i) = 2/3*(m(26,2))*(1-d2(i));
if mleach52(i) < 0
    mleach52(i) =0;
    end
end
    figure(1)
hold on
plot (tleach2,mleach52,'m')


for i = 1:length(c)

tleach2(i)=t(26)+t(i);
%   c1(i) = t(i)/10000;
 c3(i) = 1-((1-t(i)/1000)^(3));
%  c3(i) = 1-(sin(1/3*asin(1-2*t(i)/250))+1/2)^3;
mleach61(i) = 1/3*(m(26,3))*(1-c3(i));
if mleach61(i) < 0
    mleach61(i) =0;
    end
end

    figure(1)
hold on

plot (tleach2,mleach61,'c')

for i = 1:length(d)

   tleach2(i)=t(26)+t(i);
%   c1(i) = t(i)/10000;
 d3(i) = 1-((1-t(i)/100)^(3));
%  d3(i) = 1-(sin(1/3*asin(1-2*t(i)/50))+1/2)^3;
mleach62(i) = 2/3*(m(26,3))*(1-d3(i));
if mleach62(i) < 0
    mleach62(i) =0;
    end
end
    figure(1)
hold on
plot (tleach2,mleach62,'b')


for i = 1:length(c)

mleach661(i)= 1/3*(m(26,1))*(1-c1(i))+1/3*(m(26,2))*(1-c2(i))+ 1/3*(m(26,3))*(1-c3(i));
if mleach661(i) < 0
    mleach661(i) =0;
    end
end
figure(2)
hold on
plot (tleach2,mleach661,'k')


for i = 1:length(d)

mleach662(i)= 2/3*(m(26,1))*(1-d1(i))+2/3*(m(26,2))*(1-d2(i))+ 2/3*(m(26,3))*(1-d3(i));
if mleach662(i) < 0
    mleach662(i) =0;
    end
end
figure(2)
hold on
```

```
plot (tleach2,mleach662,'k')

figure(4)
hold on
plot (mleach662,mleach661,'y')

for i = 1:length(c)

tleach3(i)=t(30)+t(i);
%    c1(i) = t(i)/10000;
 c1(i) = 1-((1-t(i)/5000)^(3));
%  c1(i) = 1-(sin(1/3*asin(1-2*t(i)/1000))+1/2)^3;
mleach71(i) = 1/3*(m(30,1))*(1-c1(i));
if mleach71(i) < 0
    mleach71(i) =0;
    end
end

    figure(1)
hold on
plot (tleach3,mleach71,'r')

for i = 1:length(d)

   tleach3(i)=t(30)+t(i);
%    c1(i) = t(i)/10000;
 d1(i) = 1-((1-t(i)/500)^(3));
%  d1(i) = 1-(sin(1/3*asin(1-2*t(i)/200))+1/2)^3;
mleach72(i) = 2/3*(m(30,1))*(1-d1(i));
if mleach72(i) < 0
    mleach72(i) =0;
    end
end
    figure(1)
hold on
plot (tleach3,mleach72,'k')



for i = 1:length(c)

tleach3(i)=t(30)+t(i);
%    c1(i) = t(i)/10000;
 c2(i) = 1-((1-t(i)/2000)^(3));
%  c2(i) = 1-(sin(1/3*asin(1-2*t(i)/500))+1/2)^3;
mleach81(i) = 1/3*(m(30,2))*(1-c2(i));
if mleach81(i) < 0
    mleach81(i) =0;
    end
end

    figure(1)
hold on
plot (tleach3,mleach81,'y')

for i = 1:length(d)

   tleach3(i)=t(30)+t(i);
%    c1(i) = t(i)/10000;
 d2(i) = 1-((1-t(i)/200)^(3));
%  d2(i) = 1-(sin(1/3*asin(1-2*t(i)/100))+1/2)^3;
mleach82(i) = 2/3*(m(30,2))*(1-d2(i));
if mleach82(i) < 0
    mleach82(i) =0;
    end
end
    figure(1)
hold on
plot (tleach3,mleach82,'m')
```

```
for i = 1:length(c)

tleach3(i)=t(30)+t(i);
%   c1(i) = t(i)/10000;
 c3(i) = 1-((1-t(i)/1000)^(3));
%  c3(i) = 1-(sin(1/3*asin(1-2*t(i)/250))+1/2)^3;
mleach91(i) = 1/3*(m(30,3))*(1-c3(i));
if mleach91(i) < 0
    mleach91(i) =0;
    end
end

    figure(1)
hold on

plot (tleach3,mleach91,'c')

for i = 1:length(d)

   tleach3(i)=t(30)+t(i);
%   c1(i) = t(i)/10000;
 d3(i) = 1-((1-t(i)/100)^(3));
% d3(i) = 1-(sin(1/3*asin(1-2*t(i)/50))+1/2)^3;
mleach92(i) = 2/3*(m(30,3))*(1-d3(i));
if mleach92(i) < 0
    mleach92(i) =0;
    end
end
    figure(1)
hold on
plot (tleach3,mleach92,'b')



for i = 1:length(c)

mleach991(i)= 1/3*(m(30,1))*(1-c1(i))+1/3*(m(30,2))*(1-c2(i))+ 1/3*(m(30,3))*(1-c3(i));
if mleach991(i) < 0
    mleach991(i) =0;
    end
end
figure(2)
hold on
plot (tleach3,mleach991,'m')


for i = 1:length(d)

mleach992(i)= 2/3*(m(30,1))*(1-d1(i))+2/3*(m(30,2))*(1-d2(i))+ 2/3*(m(30,3))*(1-d3(i));
if mleach992(i) < 0
    mleach992(i) =0;
    end
end
figure(2)
hold on
plot (tleach3,mleach992,'m')


figure(4)
hold on
plot (mleach992,mleach991,'m')

for i = 1:length(c)

tleach4(i)=t(40)+t(i);
%   c1(i) = t(i)/10000;
 c1(i) = 1-((1-t(i)/5000)^(3));
%  c1(i) = 1-(sin(1/3*asin(1-2*t(i)/1000))+1/2)^3;
mleach101(i) = 1/3*(m(40,1))*(1-c1(i));
if mleach101(i) < 0
    mleach101(i) =0;
```

```
    end
end

    figure(1)
hold on
plot (tleach4,mleach101,'r')

for i = 1:length(d)

   tleach4(i)=t(40)+t(i);
%    c1(i) = t(i)/10000;
 d1(i) = 1-((1-t(i)/500)^(3));
%  d1(i) = 1-(sin(1/3*asin(1-2*t(i)/200))+1/2)^3;
mleach102(i) = 2/3*(m(40,1))*(1-d1(i));
if mleach102(i) < 0
    mleach102(i) =0;
    end
end
    figure(1)
hold on
plot (tleach4,mleach102,'k')


for i = 1:length(c)

tleach4(i)=t(40)+t(i);
%    c1(i) = t(i)/10000;
 c2(i) = 1-((1-t(i)/2000)^(3));
%  c2(i) = 1-(sin(1/3*asin(1-2*t(i)/500))+1/2)^3;
mleach111(i) = 1/3*(m(40,2))*(1-c2(i));
if mleach111(i) < 0
    mleach111(i) =0;
    end
end

    figure(1)
hold on
plot (tleach4,mleach111,'y')

for i = 1:length(d)

   tleach4(i)=t(40)+t(i);
%    c1(i) = t(i)/10000;
 d2(i) = 1-((1-t(i)/200)^(3));
%  d2(i) = 1-(sin(1/3*asin(1-2*t(i)/100))+1/2)^3;
mleach112(i) = 2/3*(m(40,2))*(1-d2(i));
if mleach112(i) < 0
    mleach112(i) =0;
    end
end
    figure(1)
hold on
plot (tleach4,mleach112,'m')


for i = 1:length(c)

tleach4(i)=t(40)+t(i);
%    c1(i) = t(i)/10000;
 c3(i) = 1-((1-t(i)/1000)^(3));
%  c3(i) = 1-(sin(1/3*asin(1-2*t(i)/250))+1/2)^3;
mleach121(i) = 1/3*(m(40,3))*(1-c3(i));
if mleach121(i) < 0
    mleach121(i) =0;
    end
end

    figure(1)
hold on
```

```
plot (tleach4,mleach121,'c')

for i = 1:length(d)

   tleach4(i)=t(40)+t(i);
%   c1(i) = t(i)/10000;
 d3(i) = 1-((1-t(i)/100)^(3));
% d3(i) = 1-(sin(1/3*asin(1-2*t(i)/50))+1/2)^3;
mleach122(i) = 2/3*(m(40,3))*(1-d3(i));
if mleach122(i) < 0
    mleach122(i) =0;
    end
end
    figure(1)
hold on
plot (tleach4,mleach122,'b')



for i = 1:length(c)

mleach1221(i)= 1/3*(m(40,1))*(1-c1(i))+1/3*(m(40,2))*(1-c2(i))+ 1/3*(m(40,3))*(1-c3(i));
if mleach1221(i) < 0
    mleach1221(i) =0;
    end
end
figure(2)
hold on
plot (tleach4,mleach1221,'b')


for i = 1:length(d)

mleach1222(i)= 2/3*(m(40,1))*(1-d1(i))+2/3*(m(40,2))*(1-d2(i))+ 2/3*(m(40,3))*(1-d3(i));
if mleach1222(i) < 0
    mleach1222(i) =0;
    end
end
figure(2)
hold on
plot (tleach4,mleach1222,'b')

figure(4)
hold on
plot (mleach1222,mleach1221,'c')


for i = 1:length(c)

tleach5(i)=t(50)+t(i);
%   c1(i) = t(i)/10000;
 c1(i) = 1-((1-t(i)/5000)^(3));
%  c1(i) = 1-(sin(1/3*asin(1-2*t(i)/1000))+1/2)^3;
mleach131(i) = 1/3*(m(50,1))*(1-c1(i));
if mleach131(i) < 0
    mleach131(i) =0;
    end
end

    figure(1)
hold on
plot (tleach5,mleach131,'r')

for i = 1:length(d)

   tleach5(i)=t(50)+t(i);
%   c1(i) = t(i)/10000;
 d1(i) = 1-((1-t(i)/500)^(3));
%  d1(i) = 1-(sin(1/3*asin(1-2*t(i)/200))+1/2)^3;
mleach132(i) = 2/3*(m(50,1))*(1-d1(i));
if mleach132(i) < 0
```

```
    mleach132(i) =0;
    end
end
    figure(1)
hold on
plot (tleach5,mleach132,'k')


for i = 1:length(c)

tleach5(i)=t(50)+t(i);
%   c1(i) = t(i)/10000;
 c2(i) = 1-((1-t(i)/2000)^(3));
%  c2(i) = 1-(sin(1/3*asin(1-2*t(i)/500))+1/2)^3;
mleach141(i) = 1/3*(m(50,2))*(1-c2(i));
if mleach141(i) < 0
    mleach141(i) =0;
    end
end

    figure(1)
hold on
plot (tleach5,mleach141,'y')

for i = 1:length(d)

   tleach5(i)=t(50)+t(i);
%   c1(i) = t(i)/10000;
 d2(i) = 1-((1-t(i)/200)^(3));
% d2(i) = 1-(sin(1/3*asin(1-2*t(i)/100))+1/2)^3;
mleach142(i) = 2/3*(m(50,2))*(1-d2(i));
if mleach142(i) < 0
    mleach142(i) =0;
    end
end
    figure(1)
hold on
plot (tleach5,mleach142,'m')


for i = 1:length(c)

tleach5(i)=t(50)+t(i);
%   c1(i) = t(i)/10000;
 c3(i) = 1-((1-t(i)/1000)^(3));
%  c3(i) = 1-(sin(1/3*asin(1-2*t(i)/250))+1/2)^3;
mleach151(i) = 1/3*(m(50,3))*(1-c3(i));
if mleach151(i) < 0
    mleach151(i) =0;
    end
end

    figure(1)
hold on

plot (tleach5,mleach151,'c')

for i = 1:length(d)

   tleach5(i)=t(50)+t(i);
%   c1(i) = t(i)/10000;
 d3(i) = 1-((1-t(i)/100)^(3));
% d3(i) = 1-(sin(1/3*asin(1-2*t(i)/50))+1/2)^3;
mleach152(i) = 2/3*(m(50,3))*(1-d3(i));
if mleach152(i) < 0
    mleach152(i) =0;
    end
end
    figure(1)
hold on
```

```
plot (tleach5,mleach152,'g')


for i = 1:length(c)

mleach1551(i)= 1/3*(m(50,1))*(1-c1(i))+1/3*(m(50,2))*(1-c2(i))+ 1/3*(m(50,3))*(1-c3(i));
if mleach1551(i) < 0
    mleach1551(i) =0;
    end
end
figure(2)
hold on
plot (tleach5,mleach1551,'g')


for i = 1:length(d)

mleach1552(i)= 2/3*(m(50,1))*(1-d1(i))+2/3*(m(50,2))*(1-d2(i))+ 2/3*(m(50,3))*(1-d3(i));

if mleach1552(i) < 0
    mleach1552(i) =0;
end
end
figure(2)
hold on
plot (tleach5,mleach1552,'r')

figure(4)
hold on
plot (mleach1552,mleach1551,'g')

for i = 1:length(c)

tleach6(i)=t(60)+t(i);
%   c1(i) = t(i)/10000;
 c1(i) = 1-((1-t(i)/5000)^(3));
%  c1(i) = 1-(sin(1/3*asin(1-2*t(i)/1000))+1/2)^3;
mleach161(i) = 1/3*(m(60,1))*(1-c1(i));
if mleach161(i) < 0
    mleach161(i) =0;
    end
end

    figure(1)
hold on
plot (tleach6,mleach161,'r')

for i = 1:length(d)

   tleach6(i)=t(60)+t(i);
%   c1(i) = t(i)/10000;
 d1(i) = 1-((1-t(i)/500)^(3));
%  d1(i) = 1-(sin(1/3*asin(1-2*t(i)/200))+1/2)^3;
mleach162(i) = 2/3*(m(60,1))*(1-d1(i));
if mleach162(i) < 0
    mleach162(i) =0;
    end
end
    figure(1)
hold on
plot (tleach6,mleach162,'k')


for i = 1:length(c)

tleach6(i)=t(60)+t(i);
%   c1(i) = t(i)/10000;
 c2(i) = 1-((1-t(i)/2000)^(3));
%  c2(i) = 1-(sin(1/3*asin(1-2*t(i)/500))+1/2)^3;
```

```
mleach171(i) = 1/3*(m(60,2))*(1-c2(i));
if mleach171(i) < 0
    mleach171(i) =0;
    end
end

    figure(1)
hold on
plot (tleach6,mleach171,'y')

for i = 1:length(d)

   tleach6(i)=t(60)+t(i);
%   c1(i) = t(i)/10000;
 d2(i) = 1-((1-t(i)/200)^(3));
%  d2(i) = 1-(sin(1/3*asin(1-2*t(i)/100))+1/2)^3;
mleach172(i) = 2/3*(m(60,2))*(1-d2(i));
if mleach172(i) < 0
    mleach172(i) =0;
    end
end
    figure(1)
hold on
plot (tleach6,mleach172,'m')


for i = 1:length(c)

tleach6(i)=t(60)+t(i);
%   c1(i) = t(i)/10000;
 c3(i) = 1-((1-t(i)/1000)^(3));
%  c3(i) = 1-(sin(1/3*asin(1-2*t(i)/250))+1/2)^3;
mleach181(i) = 1/3*(m(60,3))*(1-c3(i));
if mleach181(i) < 0
    mleach181(i) =0;
    end
end

    figure(1)
hold on

plot (tleach6,mleach181,'c')

for i = 1:length(d)

   tleach6(i)=t(60)+t(i);
%   c1(i) = t(i)/10000;
 d3(i) = 1-((I-t(i)/100)^(3));
% d3(i) = 1-(sin(1/3*asin(1-2*t(i)/50))+1/2)^3;
mleach182(i) = 2/3*(m(60,3))*(1-d3(i));
if mleach182(i) < 0
    mleach182(i) =0;
    end
end
    figure(1)
hold on
plot (tleach6,mleach182,'b')


for i = 1:length(c)

mleach1881(i)= 1/3*(m(60,1))*(1-c1(i))+1/3*(m(60,2))*(1-c2(i))+ 1/3*(m(60,3))*(1-c3(i));
if mleach1881(i) < 0
    mleach1881(i) =0;
    end
end
figure(2)
hold on
plot (tleach6,mleach1881,'k')
```

```
for i = 1:length(d)

mleach1882(i)= 2/3*(m(60,1))*(1-d1(i))+2/3*(m(60,2))*(1-d2(i))+ 2/3*(m(60,3))*(1-d3(i));
if mleach1882(i) < 0
    mleach1882(i) =0;
    end
end
figure(2)
hold on
plot (tleach6,mleach1882,'k')

figure(4)
hold on
plot (mleach1882,mleach1881,'k')

for i = 1:length(c)

tleach7(i)=t(70)+t(i);
%   c1(i) = t(i)/10000;
 c1(i) = 1-((1-t(i)/5000)^(3));
%  c1(i) = 1-(sin(1/3*asin(1-2*t(i)/1000))+1/2)^3;
mleach191(i) = 1/3*(m(70,1))*(1-c1(i));
if mleach191(i) < 0
    mleach191(i) =0;
    end
end

    figure(1)
hold on
plot (tleach7,mleach191,'r')

for i = 1:length(d)

   tleach7(i)=t(70)+t(i);
%   c1(i) = t(i)/10000;
 d1(i) = 1-((1-t(i)/500)^(3));
%  d1(i) = 1-(sin(1/3*asin(1-2*t(i)/200))+1/2)^3;
mleach192(i) = 2/3*(m(70,1))*(1-d1(i));
if mleach192(i) < 0
    mleach192(i) =0;
    end
end
    figure(1)
hold on
plot (tleach7,mleach192,'k')



for i = 1:length(c)

tleach7(i)=t(70)+t(i);
%   c1(i) = t(i)/10000;
 c2(i) = 1-((1-t(i)/2000)^(3));
%  c2(i) = 1-(sin(1/3*asin(1-2*t(i)/500))+1/2)^3;
mleach201(i) = 1/3*(m(70,2))*(1-c2(i));
if mleach201(i) < 0
    mleach201(i) =0;
    end
end

    figure(1)
hold on
plot (tleach7,mleach201,'y')

for i = 1:length(d)

   tleach7(i)=t(70)+t(i);
%   c1(i) = t(i)/10000;
 d2(i) = 1-((1-t(i)/200)^(3));
%  d2(i) = 1-(sin(1/3*asin(1-2*t(i)/100))+1/2)^3;
```

```
mleach202(i) = 2/3*(m(70,2))*(1-d2(i));
if mleach202(i) < 0
    mleach202(i) =0;
    end
end
    figure(1)
hold on
plot (tleach7,mleach202,'m')


for i = 1:length(c)

tleach7(i)=t(70)+t(i);
%   c1(i) = t(i)/10000;
 c3(i) = 1-((1-t(i)/1000)^(3));
%  c3(i) = 1-(sin(1/3*asin(1-2*t(i)/250))+1/2)^3;
mleach211(i) = 1/3*(m(70,3))*(1-c3(i));
if mleach211(i) < 0
    mleach211(i) =0;
    end
end

    figure(1)
hold on

plot (tleach7,mleach211,'c')

for i = 1:length(d)

   tleach7(i)=t(70)+t(i);
%   c1(i) = t(i)/10000;
 d3(i) = 1-((1-t(i)/100)^(3));
%  d3(i) = 1-(sin(1/3*asin(1-2*t(i)/50))+1/2)^3;
mleach212(i) = 2/3*(m(70,3))*(1-d3(i));
if mleach212(i) < 0
    mleach212(i) =0;
    end
end
    figure(1)
hold on
plot (tleach7,mleach212,'b')



for i = 1:length(c)

mleach2111(i)= 1/3*(m(70,1))*(1-c1(i))+1/3*(m(70,2))*(1-c2(i))+ 1/3*(m(70,3))*(1-c3(i));
if mleach2111(i) < 0
    mleach2111(i) =0;
    end
end
figure(2)
hold on
plot (tleach7,mleach2111,'b')


for i = 1:length(d)

mleach2112(i)= 2/3*(m(70,1))*(1-d1(i))+2/3*(m(70,2))*(1-d2(i))+ 2/3*(m(70,3))*(1-d3(i));
if mleach2112(i) < 0
    mleach2112(i) =0;
    end
end
figure(2)
hold on
plot (tleach7,mleach2112,'b')

figure(4)
hold on
plot (mleach2112,mleach2111,'b')
```

```
for i = 1:length(c)

tleach8(i)=t(80)+t(i);
%    c1(i) = t(i)/10000;
 c1(i) = 1-((1-t(i)/5000)^(3));
%  c1(i) = 1-(sin(1/3*asin(1-2*t(i)/1000))+1/2)^3;
mleach221(i) = 1/3*(m(80,1))*(1-c1(i));
if mleach221(i) < 0
    mleach221(i) =0;
    end
end

    figure(1)
hold on
plot (tleach8,mleach221,'r')

for i = 1:length(d)

   tleach8(i)=t(80)+t(i);
%    c1(i) = t(i)/10000;
 d1(i) = 1-((1-t(i)/500)^(3));
%  d1(i) = 1-(sin(1/3*asin(1-2*t(i)/200))+1/2)^3;
mleach222(i) = 2/3*(m(80,1))*(1-d1(i));
if mleach222(i) < 0
    mleach222(i) =0;
    end
end
    figure(1)
hold on
plot (tleach8,mleach222,'k')



for i = 1:length(c)

tleach8(i)=t(80)+t(i);
%    c1(i) = t(i)/10000;
 c2(i) = 1-((1-t(i)/2000)^(3));
%  c2(i) = 1-(sin(1/3*asin(1-2*t(i)/500))+1/2)^3;
mleach231(i) = 1/3*(m(80,2))*(1-c2(i));
if mleach231(i) < 0
    mleach231(i) =0;
    end
end

    figure(1)
hold on
plot (tleach8,mleach231,'y')

for i = 1:length(d)

   tleach8(i)=t(80)+t(i);
%    c1(i) = t(i)/10000;
 d2(i) = 1-((1-t(i)/200)^(3));
% d2(i) = 1-(sin(1/3*asin(1-2*t(i)/100))+1/2)^3;
mleach232(i) = 2/3*(m(80,2))*(1-d2(i));
if mleach232(i) < 0
    mleach232(i) =0;
    end
end
    figure(1)
hold on
plot (tleach8,mleach232,'m')


for i = 1:length(c)

tleach8(i)=t(80)+t(i);
%    c1(i) = t(i)/10000;
 c3(i) = 1-((1-t(i)/1000)^(3));
%  c3(i) = 1-(sin(1/3*asin(1-2*t(i)/250))+1/2)^3;
```

```
mleach241(i) = 1/3*(m(80,3))*(1-c3(i));
if mleach241(i) < 0
    mleach241(i) =0;
    end
end

    figure(1)
hold on

plot (tleach8,mleach241,'c')

for i = 1:length(d)

   tleach8(i)=t(80)+t(i);
%    c1(i) = t(i)/10000;
 d3(i) = 1-((1-t(i)/100)^(3));
% d3(i) = 1-(sin(1/3*asin(1-2*t(i)/50))+1/2)^3;
mleach242(i) = 2/3*(m(80,3))*(1-d3(i));
if mleach242(i) < 0
    mleach242(i) =0;
    end
end
    figure(1)
hold on
plot (tleach8,mleach242,'b')



for i = 1:length(c)

mleach2441(i)= 1/3*(m(80,1))*(1-c1(i))+1/3*(m(80,2))*(1-c2(i))+ 1/3*(m(80,3))*(1-c3(i));
if mleach2441(i) < 0
    mleach2441(i) =0;
    end
end
figure(2)
hold on
plot (tleach8,mleach2441,'r')


for i = 1:length(d)

mleach2442(i)= 2/3*(m(80,1))*(1-d1(i))+2/3*(m(80,2))*(1-d2(i))+ 2/3*(m(80,3))*(1-d3(i));
if mleach2442(i) < 0
    mleach2442(i) =0;
    end
end
figure(2)
hold on
plot (tleach8,mleach2442,'r')

figure(4)
hold on
plot (mleach2442,mleach2441,'r')
```